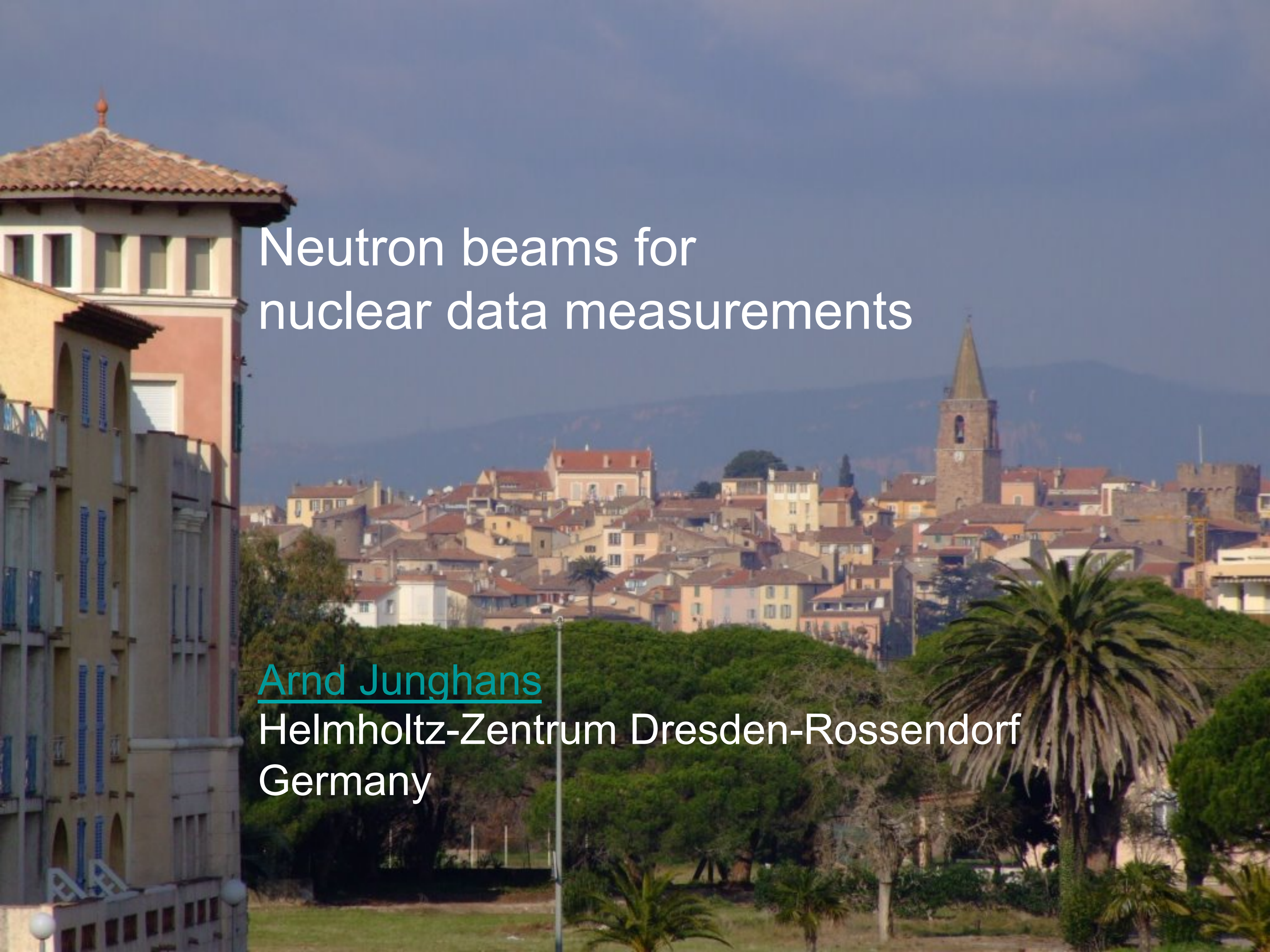

Neutron beams for nuclear data measurements

Arnd Junghans
Helmholtz-Zentrum Dresden-Rossendorf
Germany

Table of Content

- Introduction of the speaker

- Neutron sources (Terrestrial and radioisotope sources)
- Neutron producing nuclear reactions: Monoenergetic neutrons
- Kinematics e.g. $^{7}Li(p,n)^{7}Be$
- Neutron reference fields: „Big Four“ reactions for neutron production
- Neutron generators: $D(d,n)^{3}He$, $T(d,n)^{4}He$ reactions

- Time-of-flight method and neutron sources
- Spallation neutron sources using light-ion accelerators
- Slowing down of neutrons to produce eV-keV neutrons
- Photoneutron sources using electron accelerators nELBE,Gelina
- NFS at GANIL

DRESDEN concept HZDR

Schematic time of flight measurement

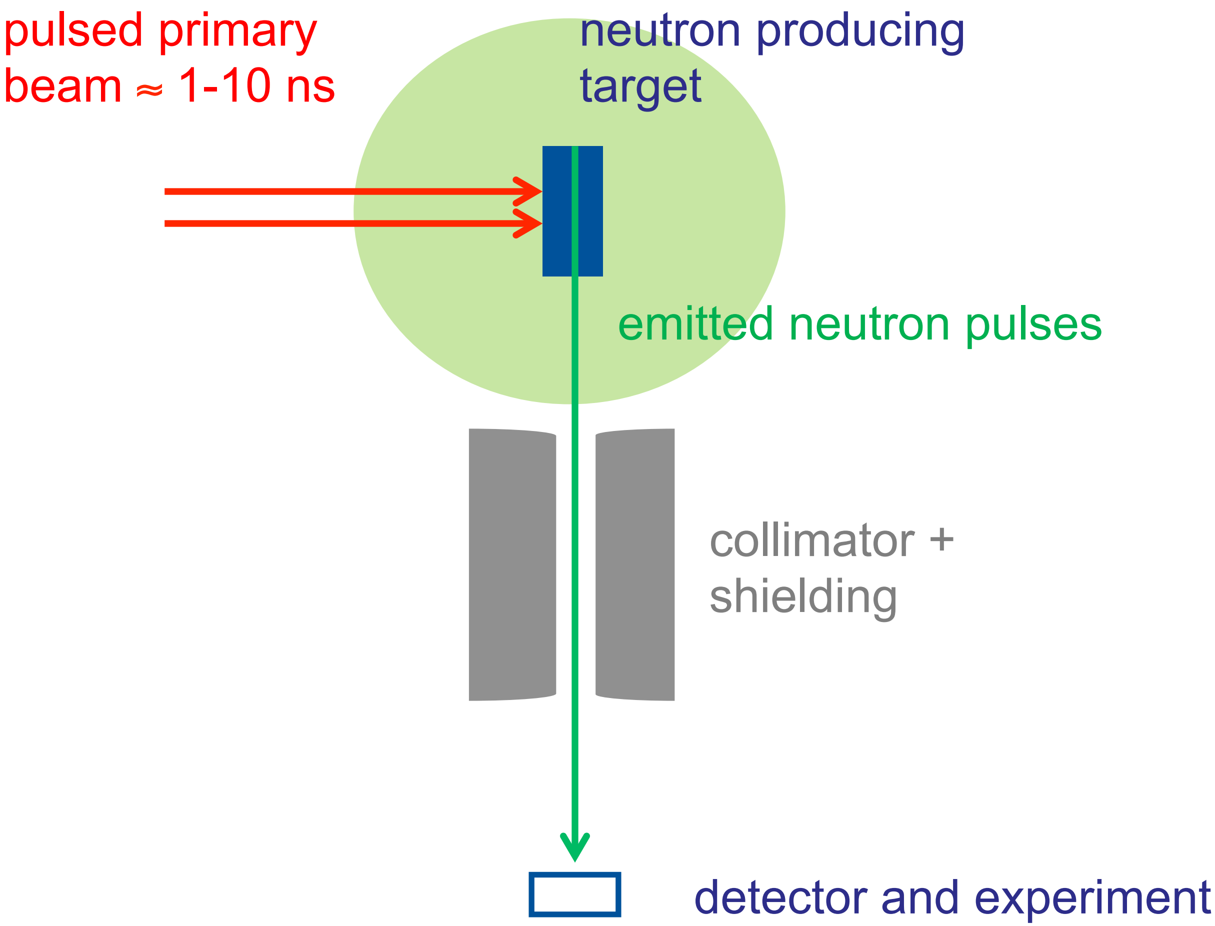

primary beams:
light charged particles with >100 MeV energy
➔ spallation neutron source

electrons 10 – 150 MeV
➔ photoneutron source

Two body kinematics ➔ quasimonochromatic neutron sources e.g. $^{7}Li(p,n)$

1-2-3 of time of flight:

- Measurement of time-of-flight t and flight path l

1. $v = l/t$
2. $\gamma = 1/\sqrt{1-(v/c)^2}$
3. $E = mc^2(\gamma - 1)$ (E is the neutron kinetic energy)

- Energy resolution

1. $\Delta E/E = (\gamma+1)\gamma\,\Delta v/v$
2. $\Delta v/v = \sqrt{(\Delta t/t)^2 + (\Delta l/l)^2}$

- accelerator pulse length, time resolution of detectors, neutron transport in the neutron producing target and detector or sample Schillebeeckx et al. NDS 113 (2012) 3054

Time-of-flight to Energy correlation

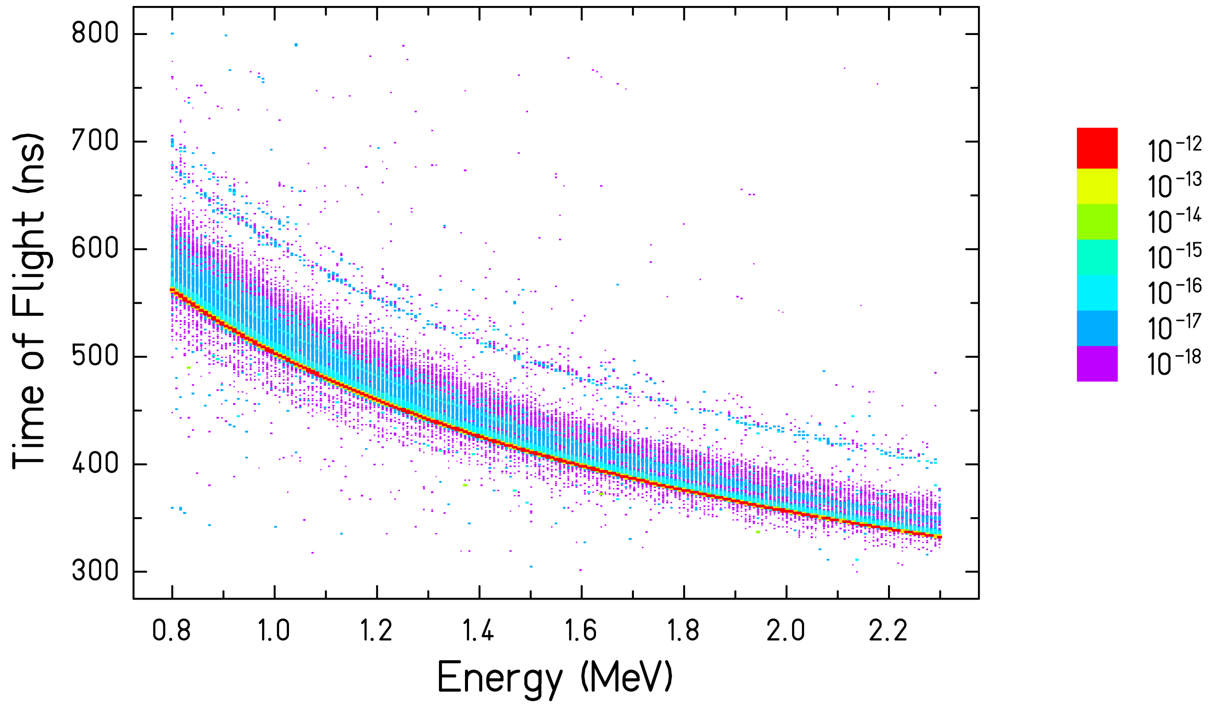

- Neutron transport code MCNP:
  Simulation of **neutron scattering** inside the neutron source and all surrounding materials e.g. collimators
- **Neutron scattering can change the correlation of time of flight and neutron energy**

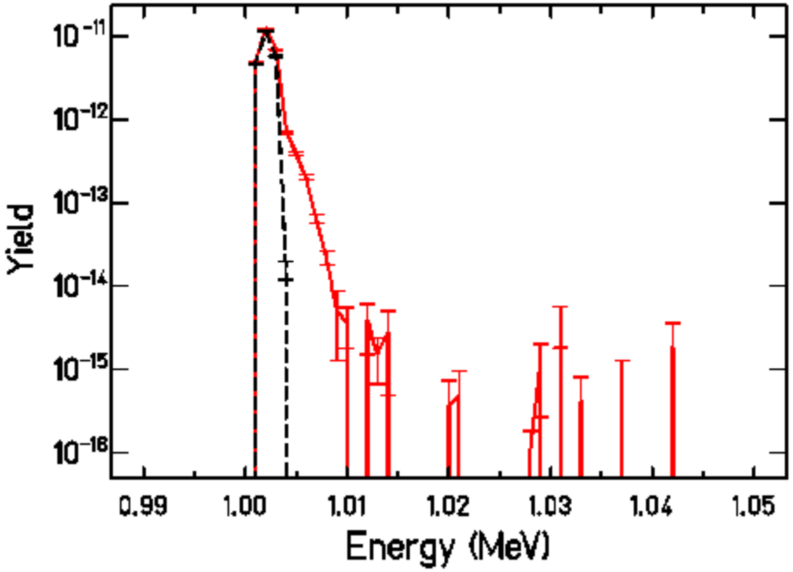

- Unscattered neutrons can be identified
  (in the simulation)

Neutron production by spallation

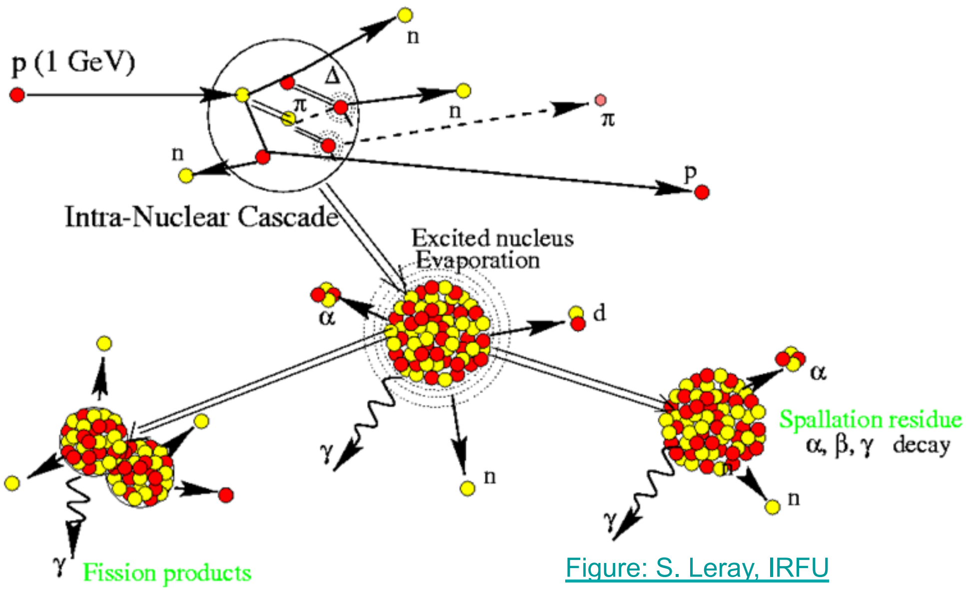

Figure: S. Leray, IRFU

Nucleon-Nucleus collisions at relativistic energies
(de Broglie wavelength < mean free path)
in two phases:

$T_{coll} < 10^{-22}$s : Collisions of the projectile nucleon with nucleons in the target (Intranuclear Cascade, emission of **fast** particles π,**n**,p,…)

$T_{equil} > 10^{-21}$s – 10^{-16}s Reorganisation of the residual nuclei, thermalization, **particle evaporation** (**n**,p,d,α,…), gamma ray emission

Spallation neutron yield

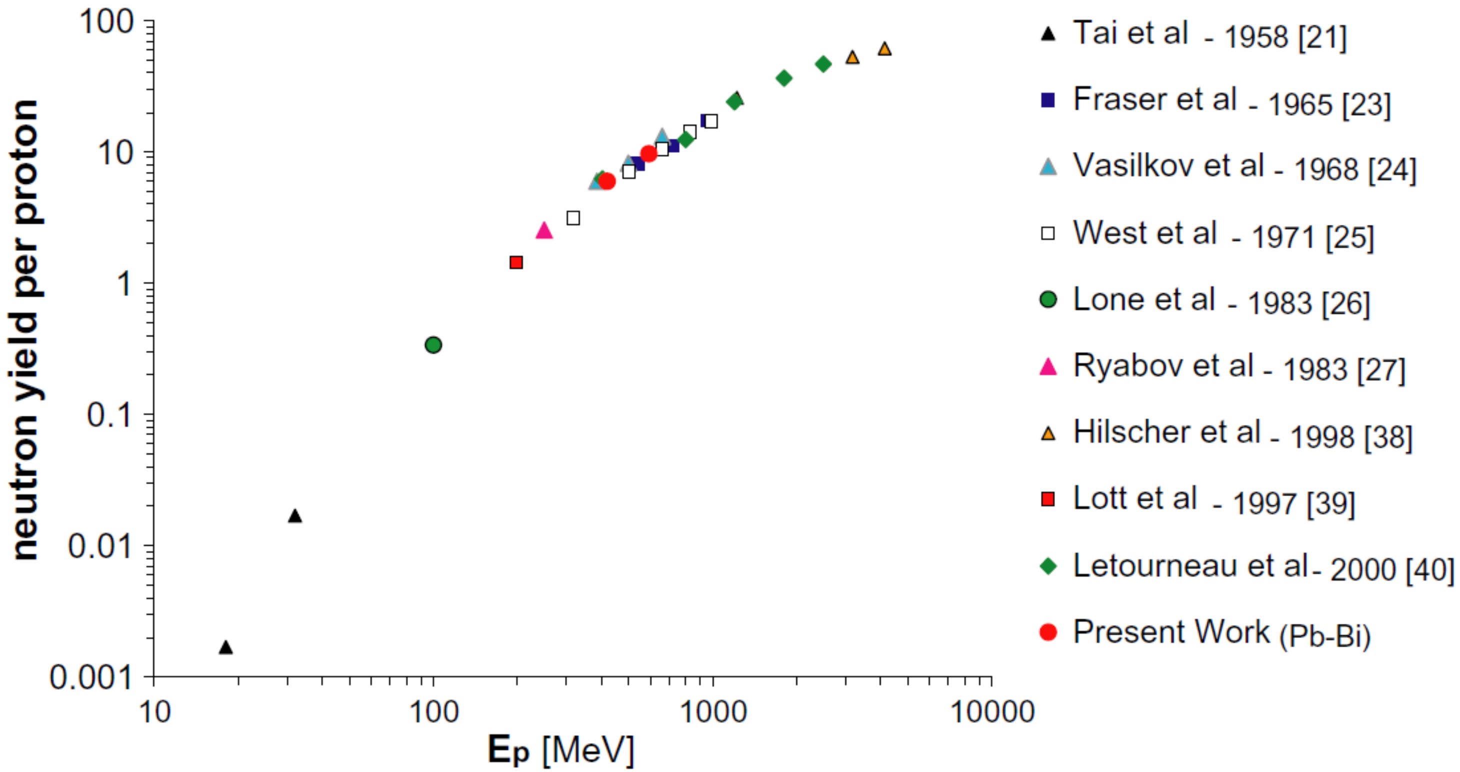

Fig. 10. Compilation of thick-target n/p values for p + Pb and Pb/Bi measured to date at all incident energies.

CERN nTOF ca. 300 n/p 20 GeV protons on Pb

K. Van der Meer, NIM B 217 (2004) 202–220

Spallation neutron spectrum at CERN nTOF

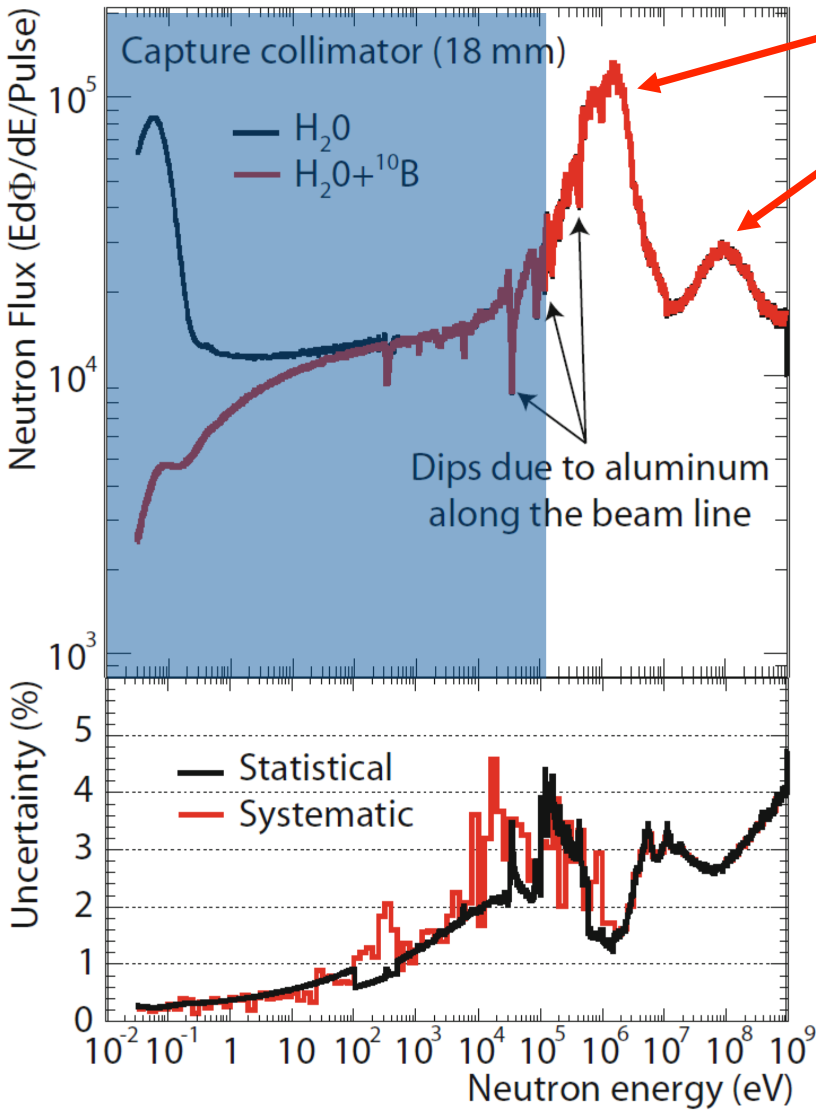

Neutron evaporation (0.1 – 10 MeV)
Fast neutrons from intranuclear cascade stage > 10 MeV

Shaded range < 0.1 MeV
Neutrons slowed down by hydrogeneous materials

CERN Proton Synchrotron 20 GeV/c

C. Guerrero et al., EPJA49 (2013) 27

Slowing down of neutrons

- Neutron transport in general: (Boltzmann equation from statistical mechanics) describes the change of Neutron number density N because of a neutron flux density gradient, neutron sources, neutron absorption or in-scattering and out-scattering
- Fundamental physics used in neutron transport theory → deterministic or stochastic (e.g. MCNP) methods to solve transport problems

$$
\begin{aligned}
\frac{\partial N(\vec{r},\vec{\Omega},E_n)}{\partial t} = \; & \frac{1}{\langle v_n \rangle}\frac{\partial \Phi(\vec{r},\vec{\Omega},E_n)}{\partial t} \\
& -\vec{\Omega}\cdot\vec{\nabla}\Phi(\vec{r},\vec{\Omega},E_n) - \Sigma_t \Phi(\vec{r},\vec{\Omega},E_n) \\
& + \int\limits_{4\pi}\int\limits_{0}^{\infty} \Sigma_s(\vec{\Omega}' \to \vec{\Omega}, \vec{E}'_n \to \vec{E}_n)\Phi(\vec{r},\vec{\Omega},E_n)\, dV' d\Omega' dE'_n \\
& + S(\vec{r},\vec{\Omega},E_n)
\end{aligned}
$$

- Q: How can we do simple tests to trust the simulation ?
  A: Simple estimates using averaged parameters
  and compare results …

Neutron transport by elastic scattering

- Neutron in a scattering medium
  no absorption, no energy change by collisions
- $x_0 = \lambda_s$ from the start the neutron moves
  on average the mean free path λ_s until first collision
- $x_1 = \lambda_s \cos\vartheta_1 = \lambda_s \mu$ projection of the path traveled in the original direction

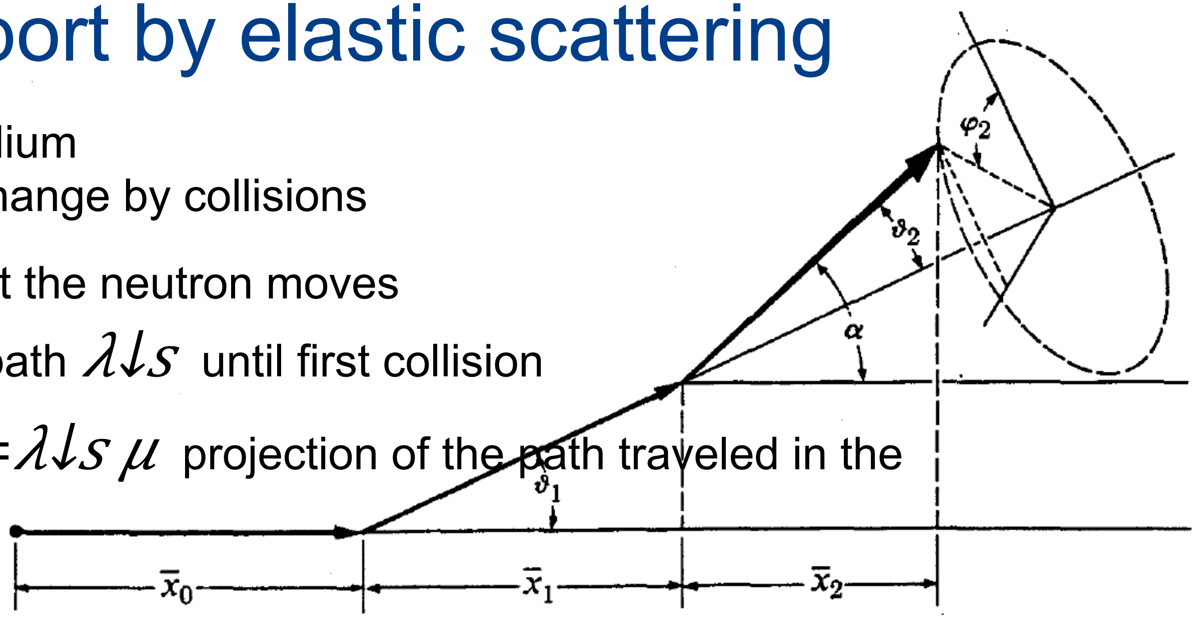

Fig. 2–22. Diagram for calculating the transport cross section.

- μ is the average value of the cosine of the scattering angle
- At the second collision: $x_2 = \lambda_s \cos\alpha$ and $\cos\alpha = \cos\vartheta_1 \cos\vartheta_2 + \sin\vartheta_1 \sin\vartheta_2 \cos\varphi_2$
- All values of φ_2 are equally probable (average value of $\sin\vartheta_1 \sin\vartheta_2 \cos\varphi_2 = 0$)

$$x_2 = \lambda_s \cos\alpha = \cos\vartheta_1 \cos\vartheta_2 = \lambda_s \mu^2 \ldots$$

➔ The average of the mean free path projection in the direction of motion approaches zero. *The neutron forgets its original direction of motion.*

J.R. Lamarsh, Introduction to Nuclear Reactor Theory, Addison-Wesley, 1966

Neutron transport by elastic scattering

- The transport mean free path $\lambda_{tr} = \lambda_s / (1-\mu)$ depends on

  μ the average value of the cosine of the scattering angle

  $$\mu = \frac{1}{\sigma_s} \int_{4\pi} \sigma_s(\vartheta) \cos\vartheta \, d\Omega = \frac{2\pi}{\sigma_s} \int_0^{\pi} \sigma_s(\vartheta) \cos\vartheta \sin\vartheta \, d\vartheta =$$

- For hydrogeneous media the scattering is **isotropic in the c.m. system** up to $E_n \approx 10$ MeV. The differential cross section is a constant $\sigma_s(\Theta_{cm}) = \sigma_s / 4\pi$

  Transformation into the C.M. system $\sigma_s(\Theta) d\Omega(\Theta) = \sigma_s(\vartheta) d\Omega(\vartheta)$

$$\mu = \frac{2\pi}{\sigma_s} \int_0^{\pi} \sigma_s(\Theta) \cos\vartheta \sin\Theta \, d\Theta = \frac{1}{2} \int_0^{\pi} \cos\vartheta \sin\Theta \, d\Theta$$

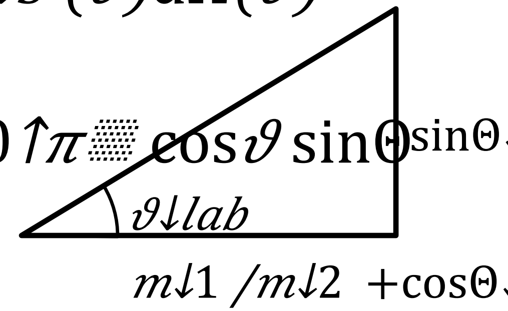

Relation of the scattering angle in the lab and c.m. system:

$$\cos\vartheta = \frac{1 + A\cos\Theta}{\sqrt{A^2 + 2A\cos\Theta + 1}}$$

	H	D	C	Fe
μ	48°	70°	87°	89°

$\mu = 2/3A$

For heavy nuclei the scattering is isotropic only below 1 MeV

Simplified scattering kernel

- Probability distribution of scattered energies
- Assumption: Isotropic scattering in the c.m. system $\sigma_s(\Theta) = \sigma_s / 4\pi$

$$W(E_n \to E_n')\,dE_n' = -2\pi \sigma_s(\Theta) \sin\Theta\, d\Theta / \sigma_s \to -\frac{1}{2} \sin\Theta\, d\Theta$$

$$W(E_n \to E_n')\,dE_n' = -W(\Theta)\,d\Theta = -W(\Theta)\frac{d\Theta}{dE_n'}\,dE_n'$$

- The energy of the scattered neutron is a function of the scattering angle:

$$\frac{dE_n'}{d\Theta} = \frac{1}{2} E_n (1-\alpha)(-\sin\Theta)\,; \alpha \stackrel{\text{def}}{=} \frac{(A-1)^2}{(A+1)^2}$$

- The scattering kernel for isotropic scattering is

$$W(E_n \to E_n') = \frac{1}{E_n(1-\alpha)}\,dE_n'$$

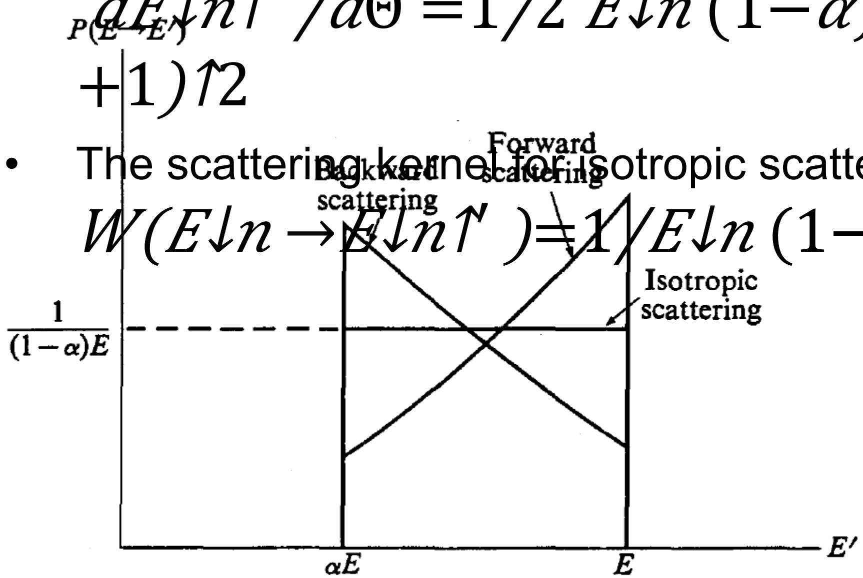

J.R. Lamarsh, Introduction to Nuclear Reactor Theory, Addison-Wesley, 1966

Average energy loss in elastic scattering and average energy of elastically scattered neutrons

- With the scattering kernel the average energy loss is:
  $$<\Delta E> = \int_{E_{min}}^{E_{max}} W(E_n \rightarrow E_n')(E_n - E_n')\, dE_n'$$

$$<\Delta E> = \int_{\alpha E_n}^{E_n} \frac{1}{E_n (1-\alpha)} (E_n - E_n')\, dE_n' = \frac{1-\alpha}{2} E_n$$

- The relative energy loss is constant: $\boldsymbol{<\Delta E>/E_n = \frac{1-\alpha}{2}}$
- Average energy of elastically scattered neutrons:
  $$<E_n'> = \int_{E_{min}}^{E_{max}} W(E_n \rightarrow E_n')(E_n')\, dE_n'$$

$$\boldsymbol{<E_n'> = E_n \frac{(1+\alpha)}{2}}$$

- The average energy of the scattered neutron is in the center of the range $[E_n, \alpha E_n]$

Further reading:
K. Wirtz, K. Beckurtz, Elementare Neutronenphysik, Springer 1958
And other literature about neutron transport theory

How many collisions are required to moderate a neutron ?

- Estimate using the lethargy $u \stackrel{\text{def}}{=} \ln E_n / E_n'$
- The average logarithmic energy loss is: $\xi = \int_{\alpha E_n}^{E_n} W(E_n \to E_n') \ln E_n / E_n'$

Special case: isotropic scattering: $\xi(\alpha) = 1 + \alpha/(1-\alpha) \ln \alpha$

- Average logarithmic energy loss ξ for hydrogen ($\alpha = 0$ as $A = 1$)

$$\lim_{\alpha \to 0} \xi(\alpha) = 1$$

- Assume initial lethargy zero. After n collisions increase of lethargy is $u_n = \sum_{i=1}^{n} \Delta u_i$.
- The average lethargy after n collisions is similar $\bar{u}_n = \sum_{i=1}^{n} \overline{\Delta u_i}$
- The average lethargy $\overline{\Delta u_i} = \xi$ ➔ $n = \bar{u}_n / \xi$
- To increase the average lethargy to the value u_n whose corresponding energy is E

$$n = 1/\xi \ln E_0 / E$$

collisions are required.

Average number of collisions to slow down neutrons …

Nuclide	A	α	ξ	n
H	1	0	1	18
D	2	0.111	0.725	25
Be	9	0.64	0.209	86
C	12	0.716	0.158	114
Fe	56	0.931	0.0353	516
U	238	0.983	0.00838	2172

- Estimated with $n = \frac{1}{\xi} \ln \frac{E_0}{E}$ assuming isotropic scattering
  $\xi(\alpha) = 1 + \frac{\alpha}{1-\alpha} \ln \alpha$
  from E_n = 2 MeV to 25 meV

Slowing down vs. Neutron capture

116 3. Nuclear reactions

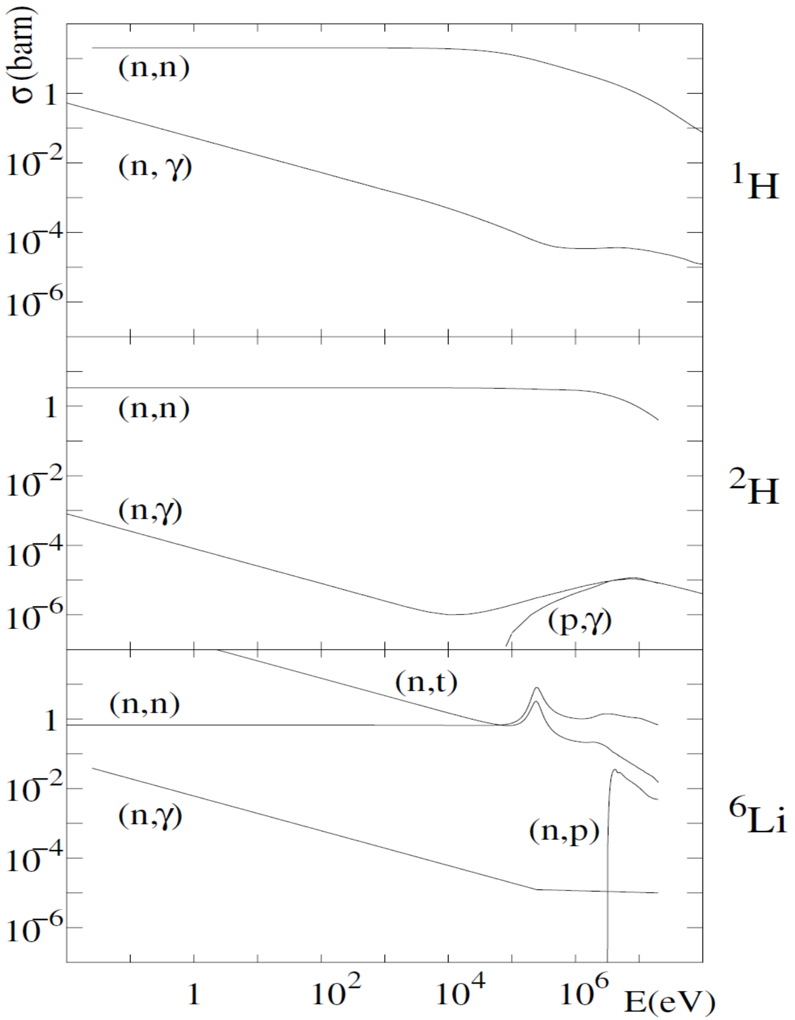

Fig. 3.4. Examples of reaction cross-sections on ^{1}H, ^{2}H, and ^{6}Li [30]. Neutron elastic scattering, (n,n), has a relatively gentle energy dependence while the exothermic reactions, (n, γ) and ^{6}Li(n, t)^{4}He (t=tritium=^{3}H), have a $1/v$ dependence at low energy. The exothermic (p, γ) reaction is suppressed at low energy because of the Coulomb barrier. The reaction ^{6}Li(n, p)^{6}Be has an energy threshold. The fourth excited state of ^{7}Li (Fig. 3.5) appears as a prominent resonance in n^{6}Li elastic scattering and in ^{6}Li(n, t)^{4}He.

Fundamentals in Nuclear Physics, J.L.Basdevant, J. Rich, J. Spiro, Springer 2005

Elastic scattering on light nuclei
Efficiently slows neutrons down.

In normal hydrogen neutron capture reduces the neutron flux density (E_γ=2.2 MeV capture gamma rays)

In deuterium the capture fraction is
Much lower

Simulation of neutron random-walk

- Monte Carlo Simulation of neutrons slowing down in hydrogeneous material e.g. Polyethylene (only hydrogen atoms take part)
  programmed in scilab by Georg Schramm, HZDR
  (similar to Matlab, Octave with graphics capabilities)

1. Neutrons start all in the same direction or isotropically.
2. Isotropic scattering angles φ, ϑ sampled for each collision
3. Calculation of energy and lab angle from kinematics relations
4. Mean free path random samples up to $5\lambda_s$ from an exponential-distribution with average value λ_s
5. Energy dependent n-p scattering cross section formula.
6. Statistical analysis of the MC results

Author: Georg Schramm, HZDR

Neutron energy loss from elastic scattering

Six simulated neutron trajectories

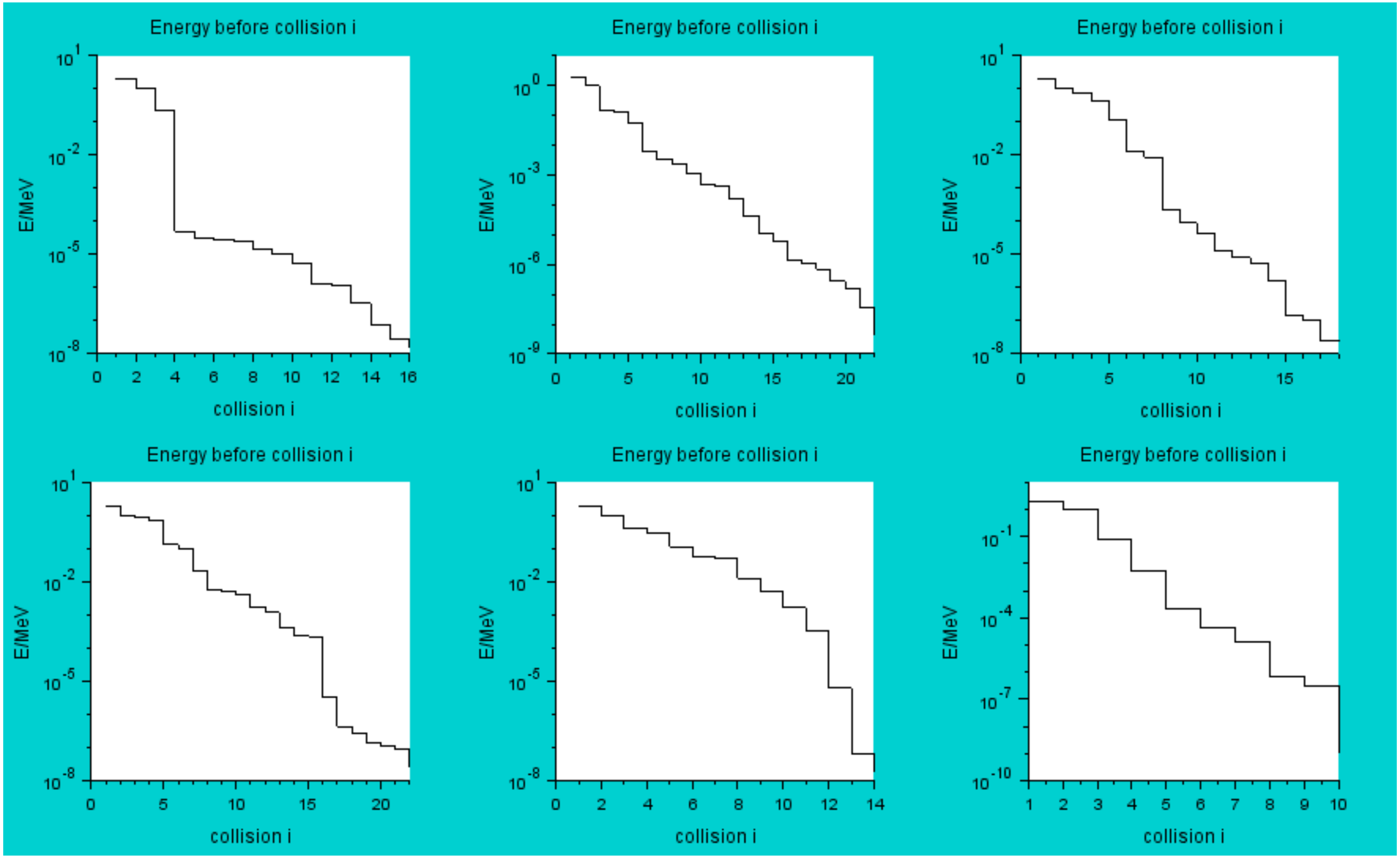

E_n = 2 MeV down to $E_{n'}$=25 meV

Scattering angle in the lab from elastic scattering

Six simulated neutron trajectories

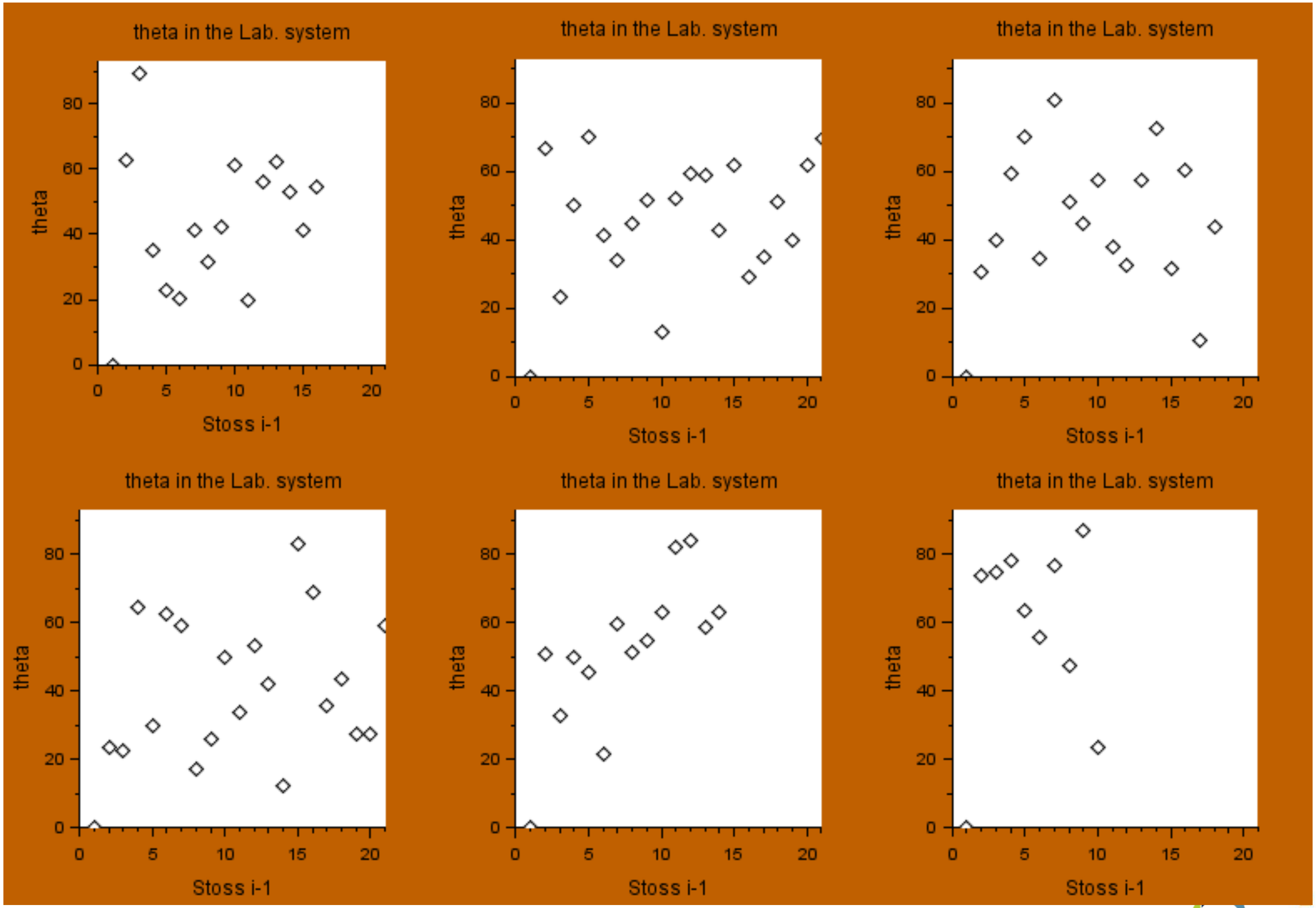

E_n = 2 MeV down to $E_{n'}$=25 meV

Scattering angle in the lab from elastic scattering

Six simulated neutron trajectories.
All neutrons start in the same direction along the positive z-axis.

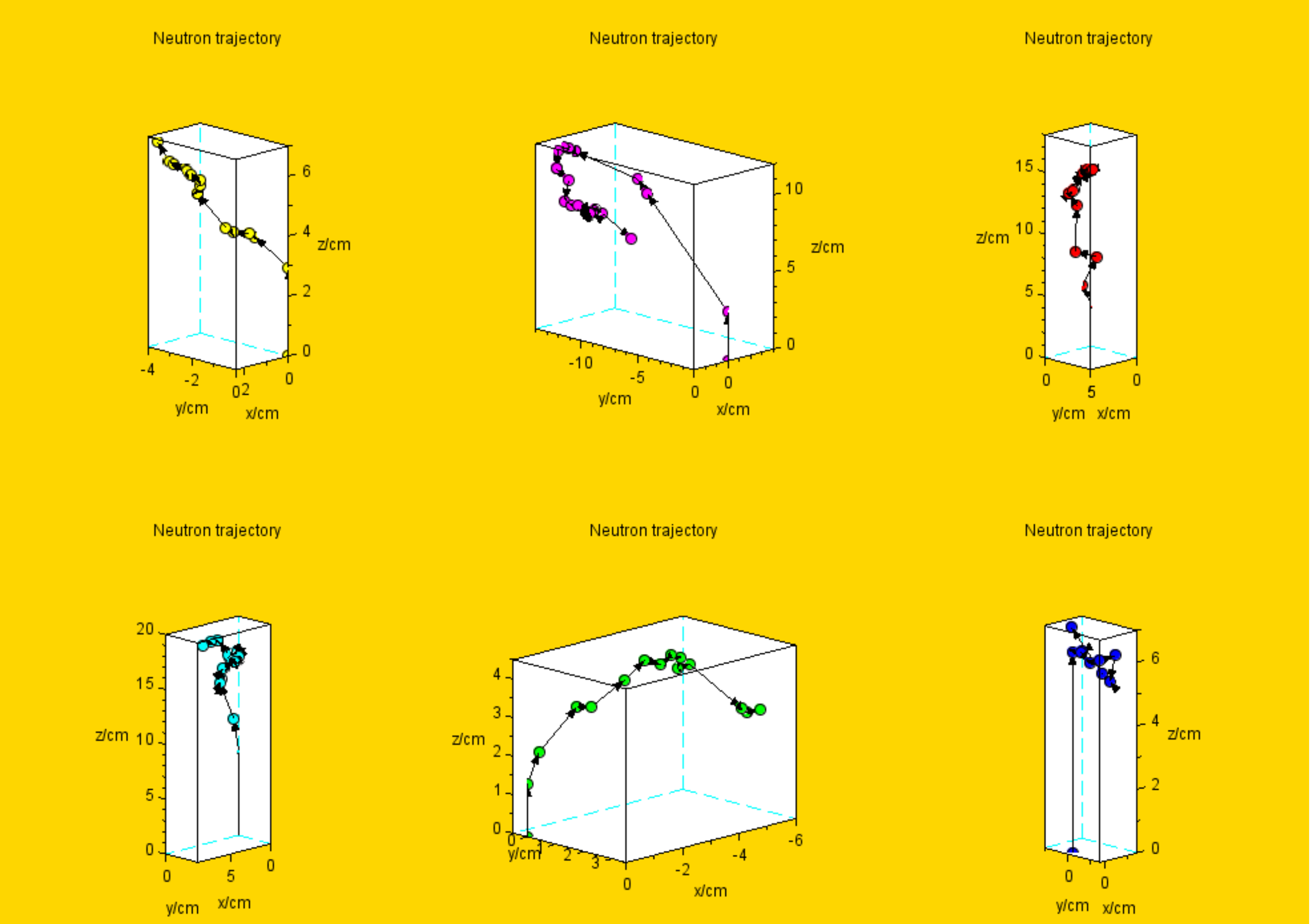

E_n = 2 MeV down to $E_{n'}$=25 meV

Scattering angle in the lab from elastic scattering

Six simulated neutron trajectories

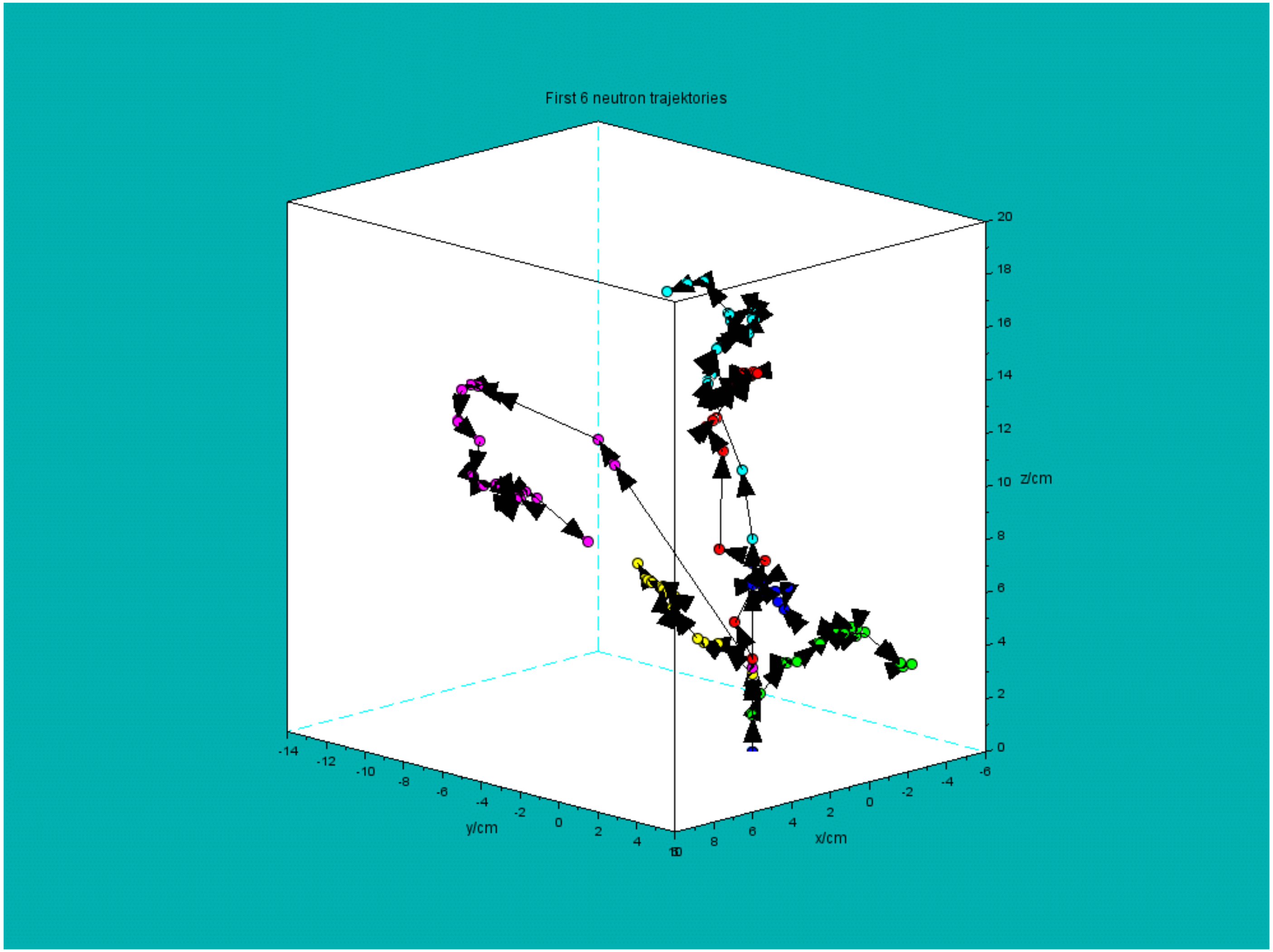

E_n = 2 MeV down to $E_{n'}$=25 meV

Points where neutrons reach thermalisation

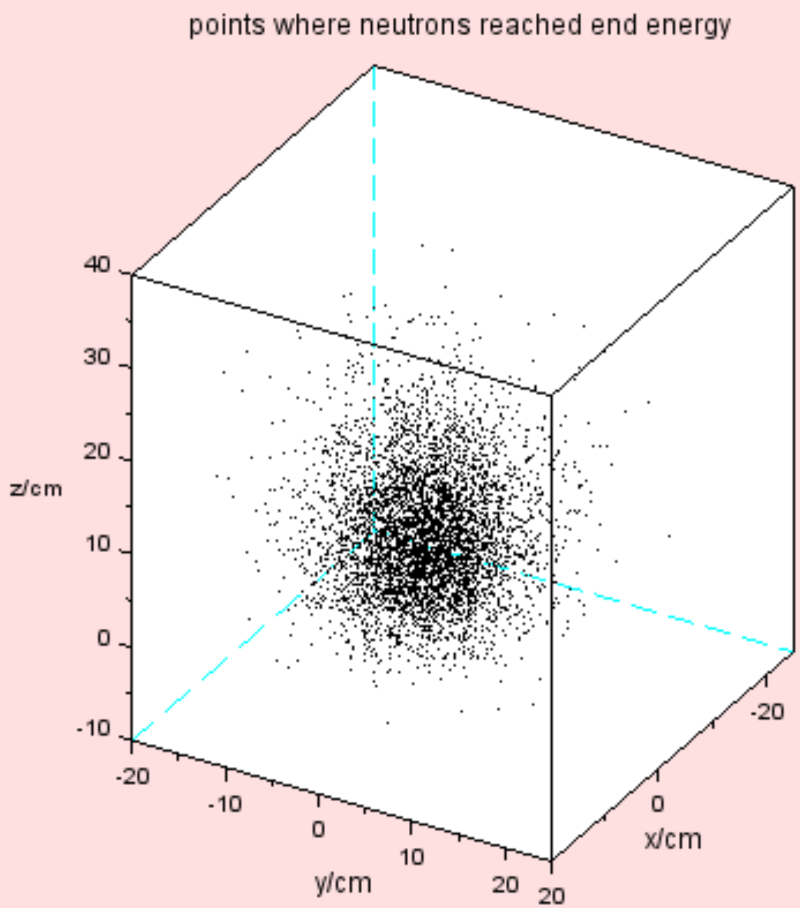

E_n = 2 MeV down to $E_{n'}$=25 meV
Neutrons have lost their initial direction.

Slowing down distance, time of moderation, number of collisions, mean free

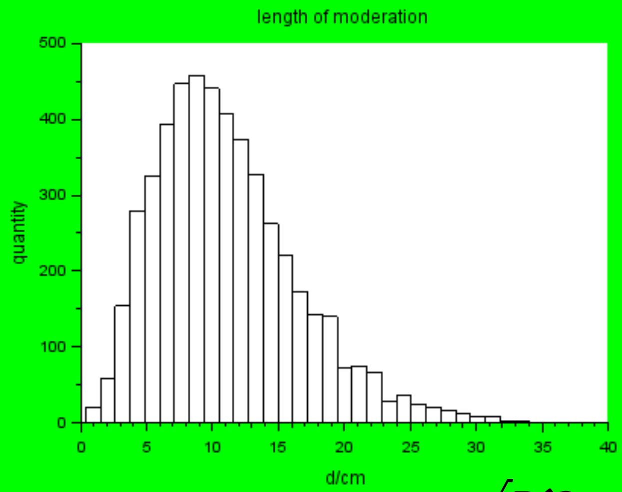

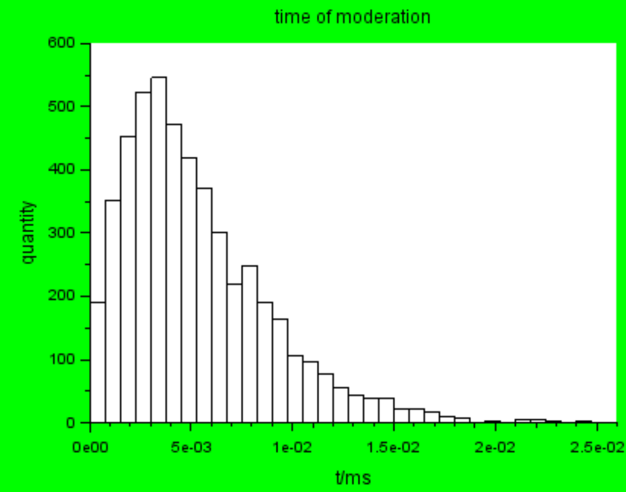

RMS slowing down distance $\sqrt{R^2} = 11.1$ cm

Average slowing down time: $5.3\ \mu$s

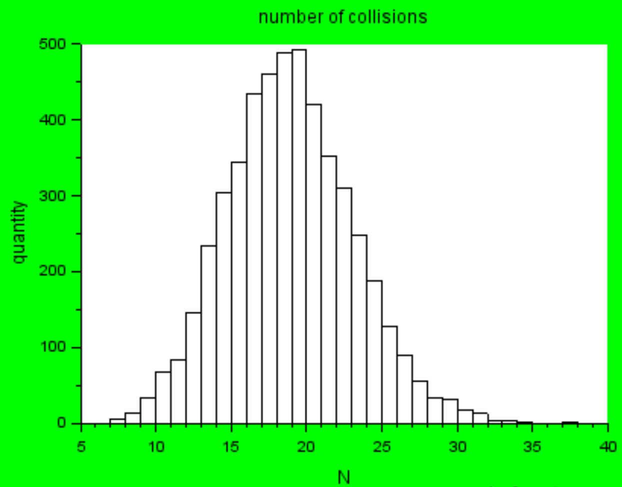

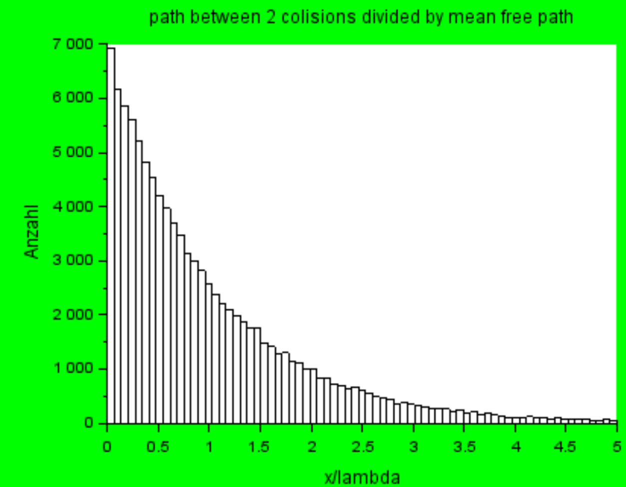

Average number of collisions: 19.4

Estimates of the slowing down distance / time

$$\langle R^2 \rangle = 2 \cdot \left[\sum_{j=1}^{n} \lambda_j^2 + \sum_{j=1}^{n-1} \lambda_j \sum_{k=j+1}^{n} \lambda_k \langle \cos\theta \rangle^{k-j} \right]$$

$$\bar{t} = \sum_{j=1}^{n} \Delta t_j = \sum_{j=1}^{n} \frac{\lambda_j}{v_j}$$

E. Fermi assumed constant mean free path: (not realistic for fast neutrons)

$$\langle R^2 \rangle = 2\lambda^2 \cdot \left[\sum_{j=1}^{n} + \sum_{j=1}^{n-1} \sum_{k=j+1}^{n} \langle \cos\theta \rangle^{k-j} \right]$$

$$\langle R^2 \rangle = \frac{2n\lambda^2}{1-\mu} \left[1 - \frac{\mu}{n} \frac{1-\mu^n}{1-\mu} \right]$$

For a comparison of „averaged“ analytical description of the random-walk and full MC
See W.J. Nellis, Am.Jour.Phys. 45 (1977) 444

Average slowing down time of 14.1 MeV Neutronen:

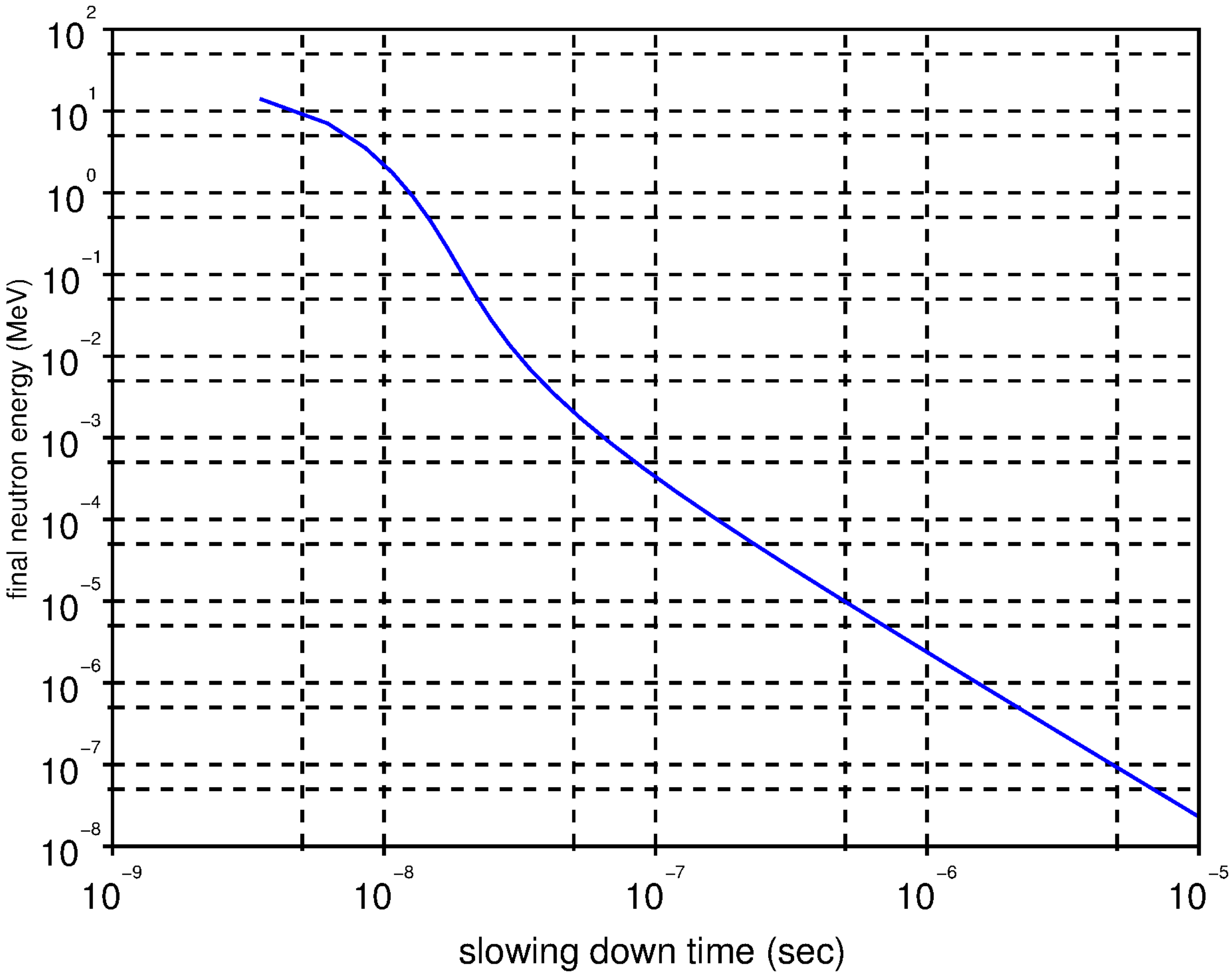

To reach thermal energy from 14 MeV takes several μs

Average slowing down distance from averaged parameters

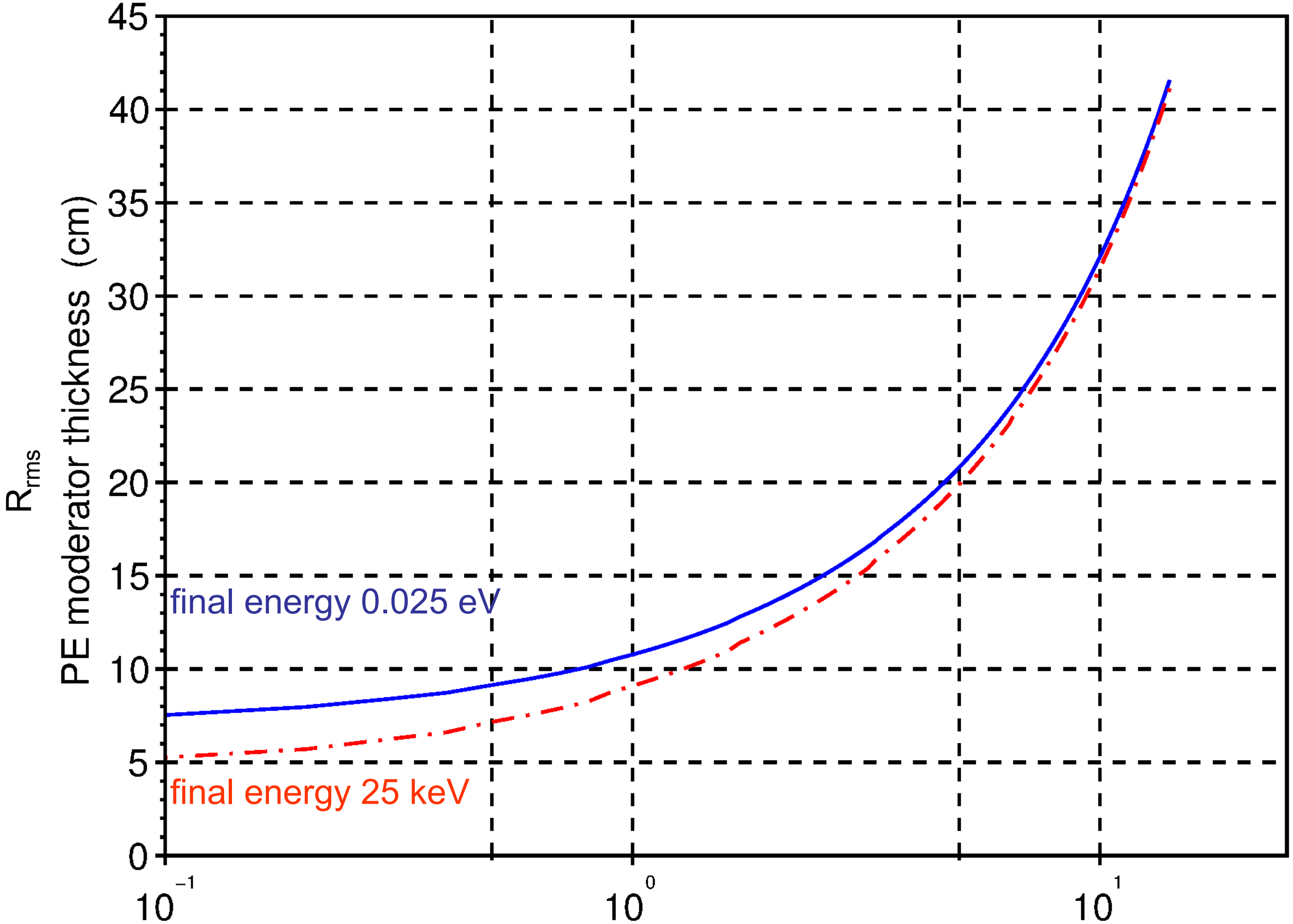

Average slowing down distance depends only weakly on the final energy required.

11 cm PE thermalize a 1 MeV Neutron
41 cm PE thermalize a 14.1 MeV Neutron

Shielding and collimation of neutrons

- Shielding and collimations of neutrons in the fast energy range **is complicated** and can even be ***very*** complicated.
- The complete experimental setup in a rather realistic geometry needs to be simulated with reliable particle transport simulations.

- A shielding needs to be thicker than the slowing down distance discussed here in order to reach an intensity reduction of 10^{-3} to 10^{-6} depending on the quality required.
- In general, all material very close to the neutron source or detector causes the most scattering and experimental background due to the large geometrical solid angle.
- Room return background of scattered neutrons from the walls, floor and ceiling is difficult to avoid and usually not negligible.

- Monte Carlo simulations for shieldings and collimators are not straightforward as very high statistical accuracy is needed to describe strong intensity reductions of several orders of magnitude.
- Simple attenuation estimates can help to test if any biasing methods in the MC simulation are adequate

DRESDEN concept

HZDR

Neutron scattering in a deuteron breakup exp.

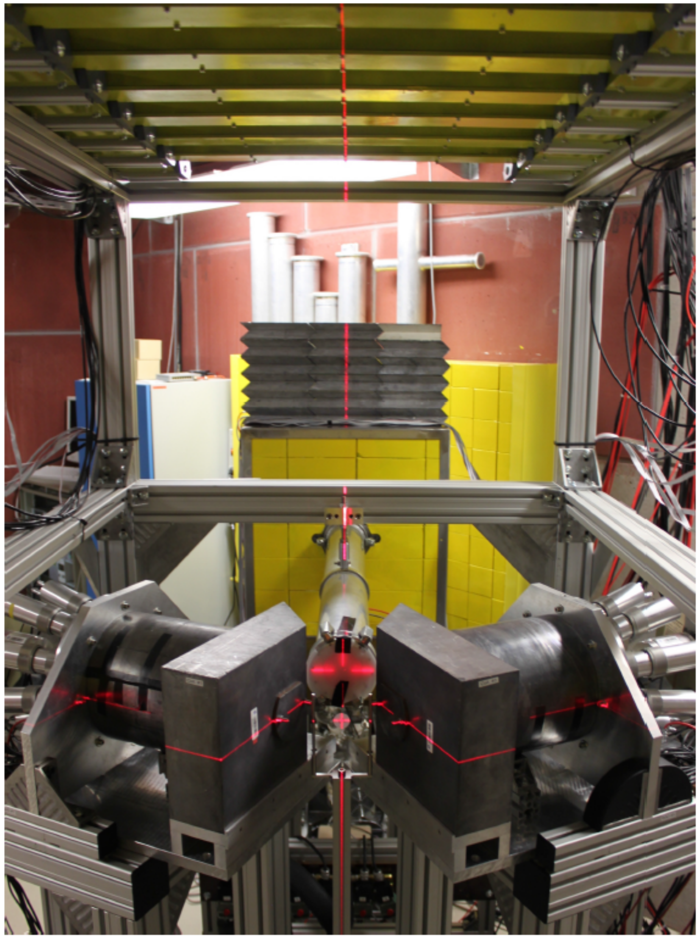

D(γ,n)H cross section measurement:
Time of flight measurement of breakup neutrons with plastic scintillators
Bremsstrahlung intensity determined by nuclear resonance fluorescence of ^{27}Al with HPGe detectors
Target 2 cm thick CD_2 with Al disks
pulsed bremsstrahlung (615 ns); end point energy 6 MeV

FLUKA simulation of the complete setup

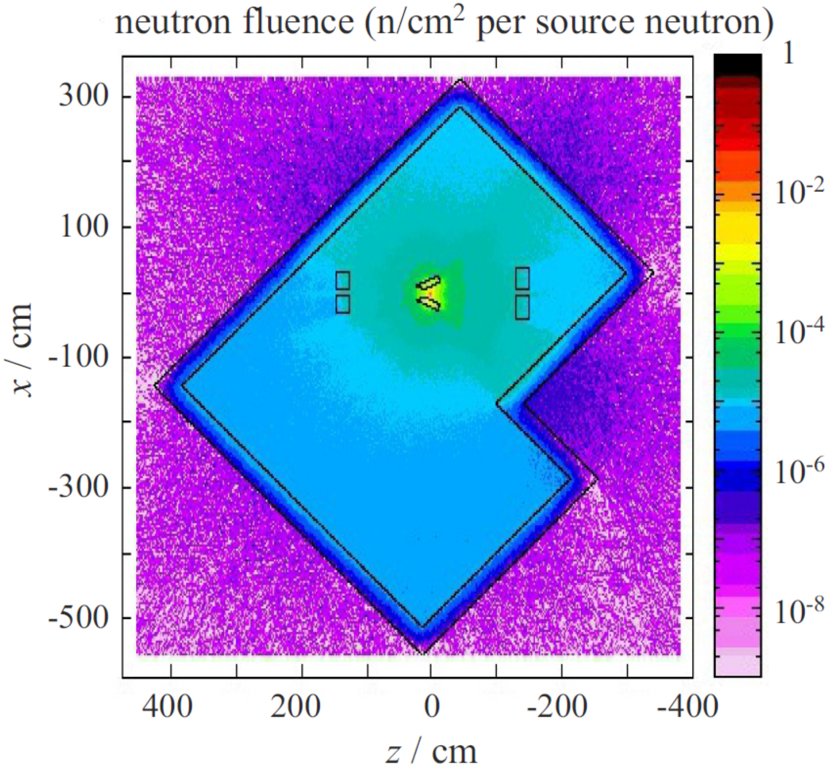

R. Hannaske, Dissertation TU Dresden, in preparation 2014

Typical neutron trajectory

3 Projections in the vertical x-y plane of the same simulated event

Neutron is slowed down in the ceiling by elastic scattering (hydrogen)
Two capture gamma-rays
scattering on atoms in the wall

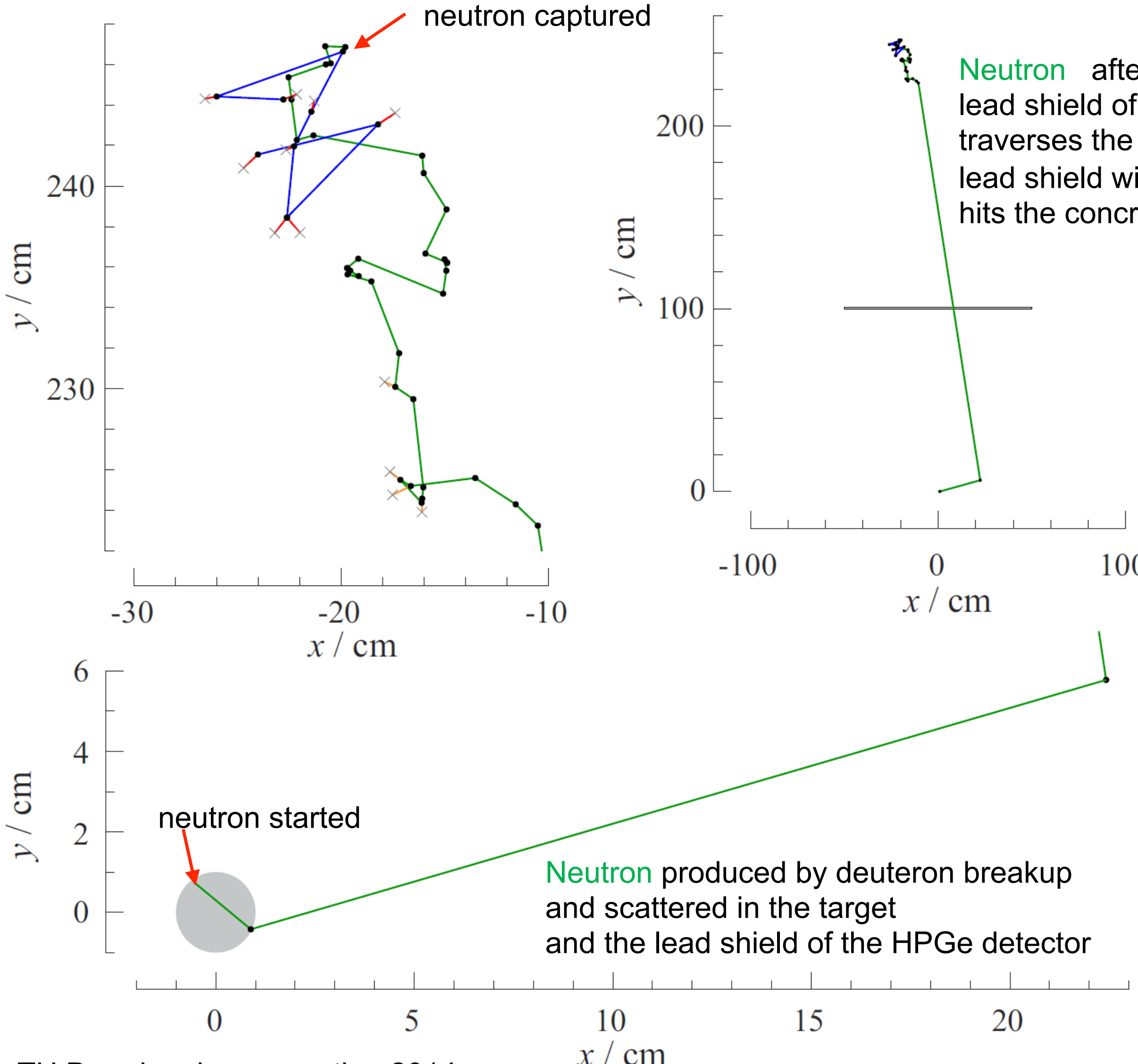

R. Hannaske, Dissertation TU Dresden, in preparation 2014

Time of flight to neutron energy correlation

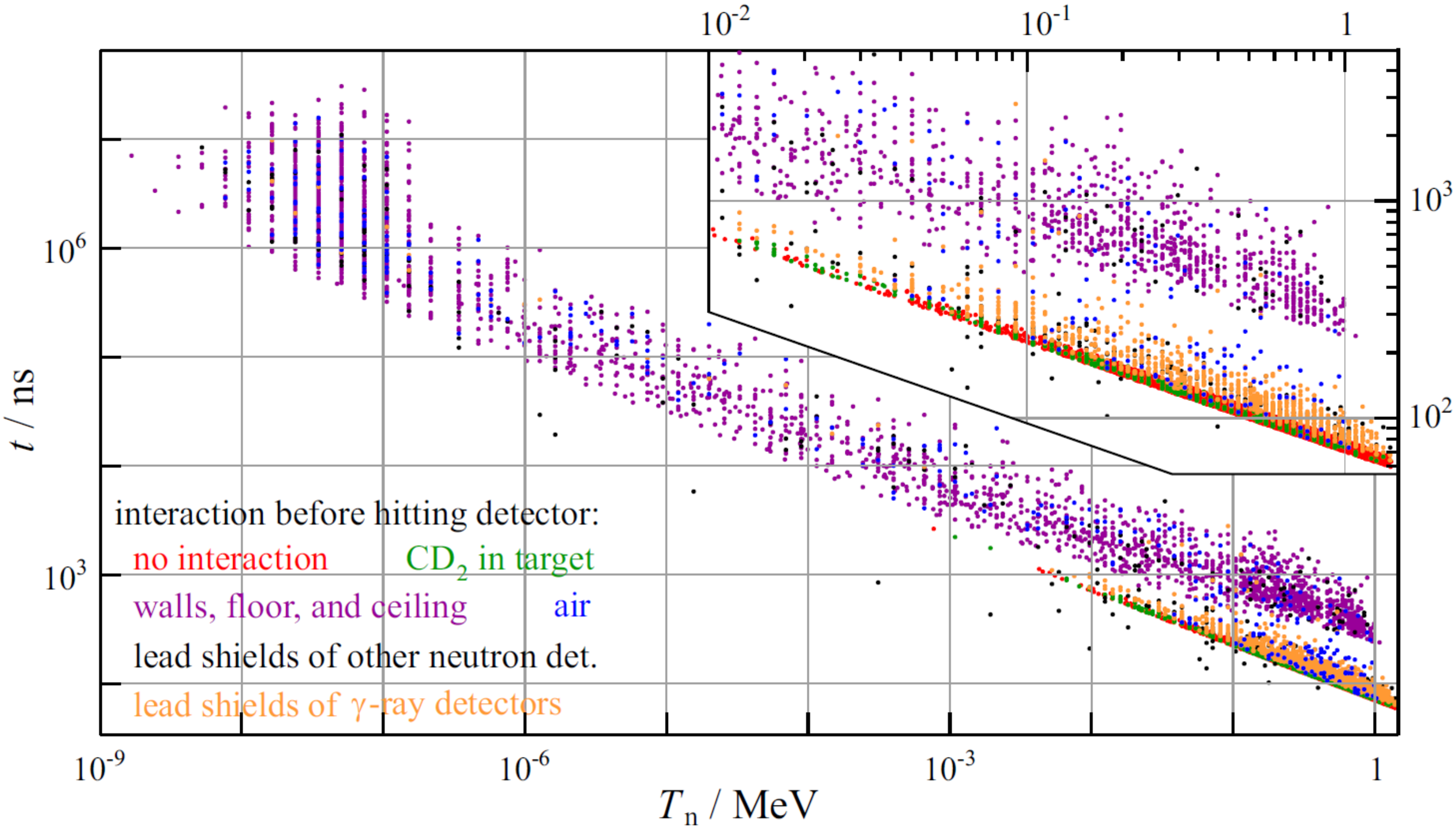

1. scattering of neutrons in the MeV range ➔ room return
2. Lead shield around HPGe is detrimental to the tof measurement.

The inset shows the range where the used detectors had sufficient efficiency

Strong neutron absorption through resonances

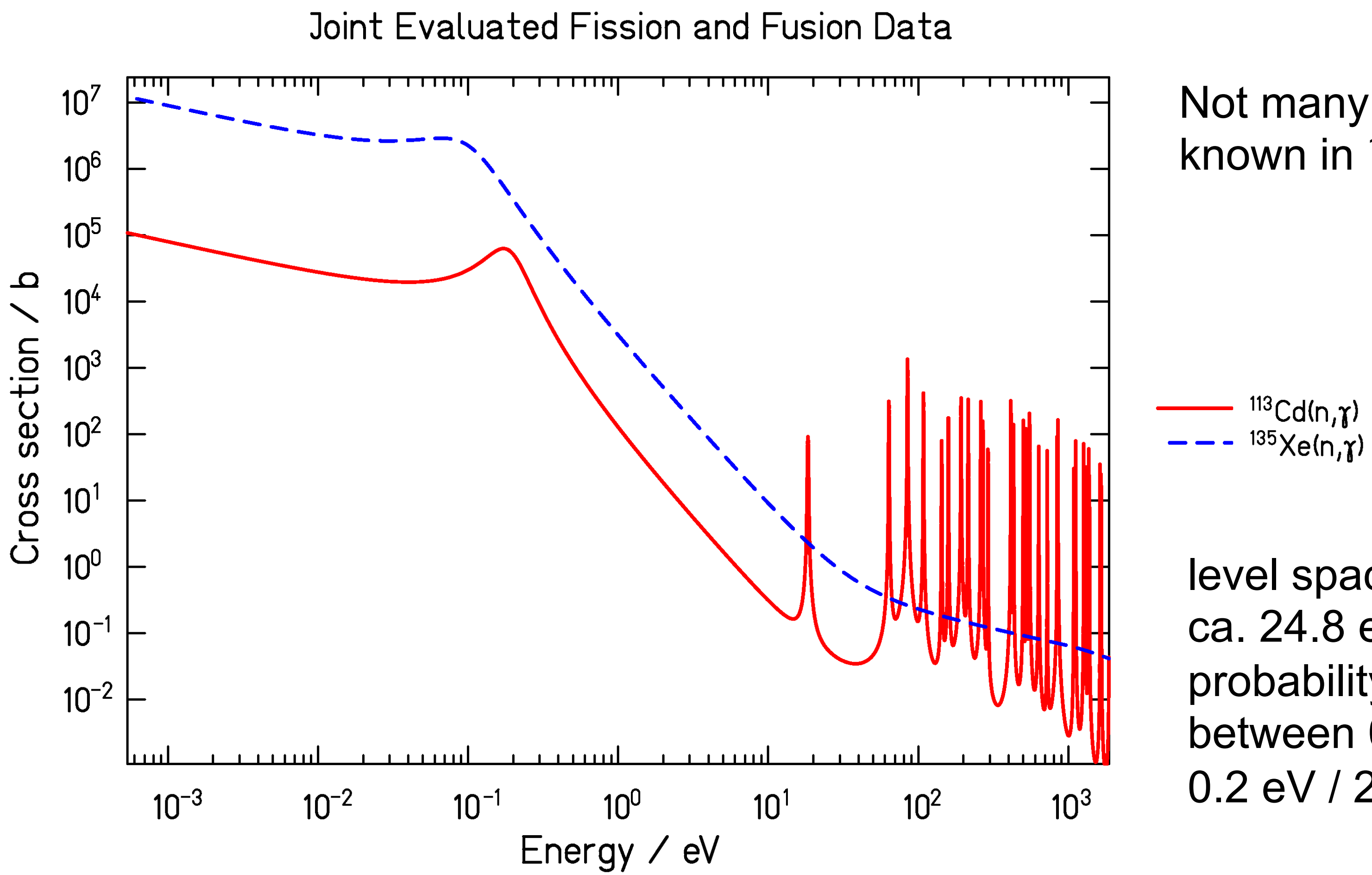

Not many resonances known in ^{135}Xe

level spacing in ^{113}Cd ca. 24.8 eV
probability for a resonance between 0-0.2 eV :
0.2 eV / 24.8 eV = 0.8 % (!)

Neutrons are slowed down by elastical scattering and then captured
The radiative neutron capture cross section rises as $1/v_n$
In some nuclides strong resonances are located close to the thermal range
e.g. ^{113}Cd+n $\sigma_{n,\gamma} = 20600$ barn, ^{135}Xe, …

CERN n_TOF Experiment

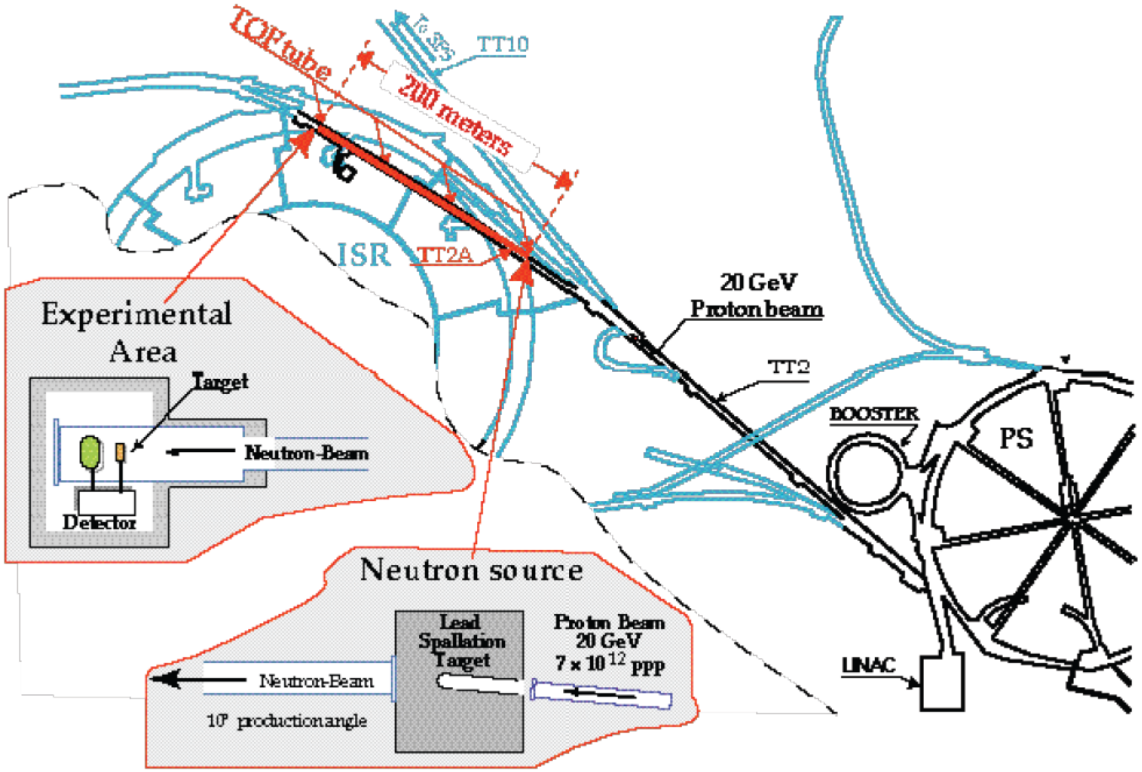

- New spallation target in 2009 ca. 300 n per proton of 20 GeV
- Radioactive target capability at experimental station

Scientific programme: nuclear astrophysics (neutron capture)

Nuclear Data measurements (neutron induced fission)

[CERN nTOF performance report](#)
CERN/INTC-O-011
INTC-2002-037
CERN-SL-2002-053 ECT

n_TOF Experimental Area 2 (EAR-2)
[CERN-INTC-2012-029](#) / INTC-O-015
will be operational in July 2014

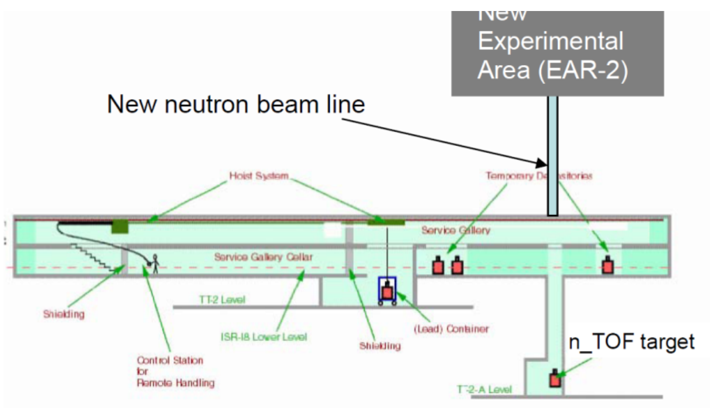

EAR-2:
short flight path 20 m
for higher intensity
90° to the proton beam
➔ Background reduction

Main characteristics of the existing n_TOF EAR-1

NEUTRON FLUX

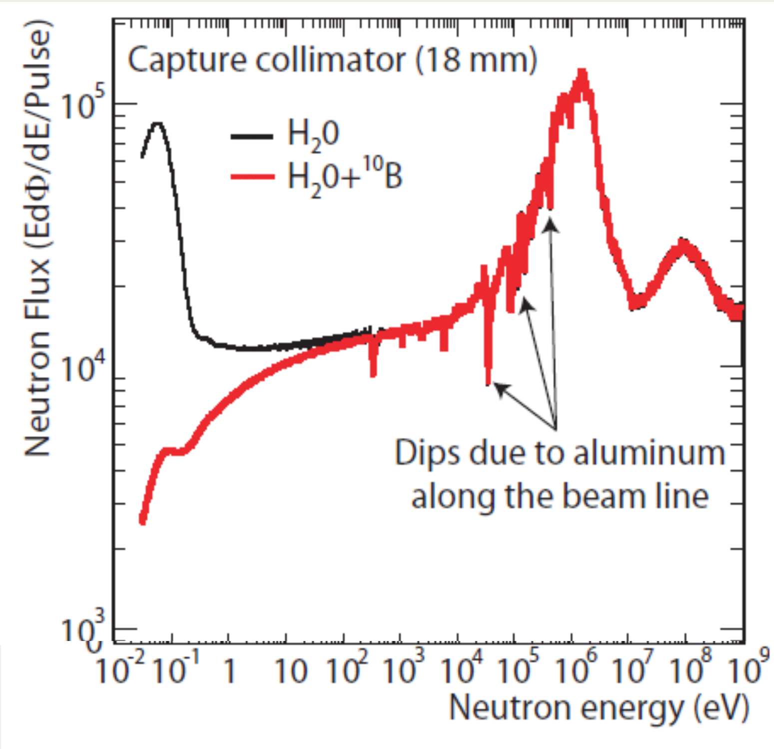

$0{,}6 \cdot 10^6$ neutrons/pulse (capture mode)
$12 \cdot 10^6$ neutrons/pulse (fission mode)

See [C. Guerrero et al. *Eur Phys. J. A 49:27 (2013)*]

BEAM PROFILE

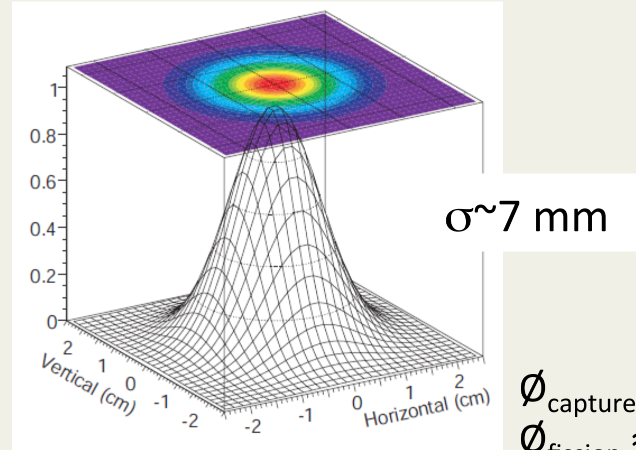

$\varnothing_{capture}$ ≈2 cm
$\varnothing_{fission}$ ≈ 8 cm

ENERGY RESOLUTION

E_n (eV)	$\Delta E_n/E_n$
1	$4.3 \cdot 10^{-4}$
10	$4.3 \cdot 10^{-4}$
10^2	$4.3 \cdot 10^{-4}$
10^3	$7.5 \cdot 10^{-4}$
10^4	$1.7 \cdot 10^{-3}$
10^5	$5.4 \cdot 10^{-3}$
10^6	$2.8 \cdot 10^{-3}$

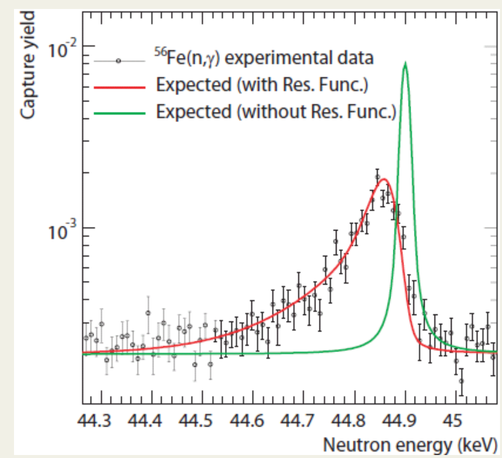

The future: n_TOF vertical flight path at 20 m

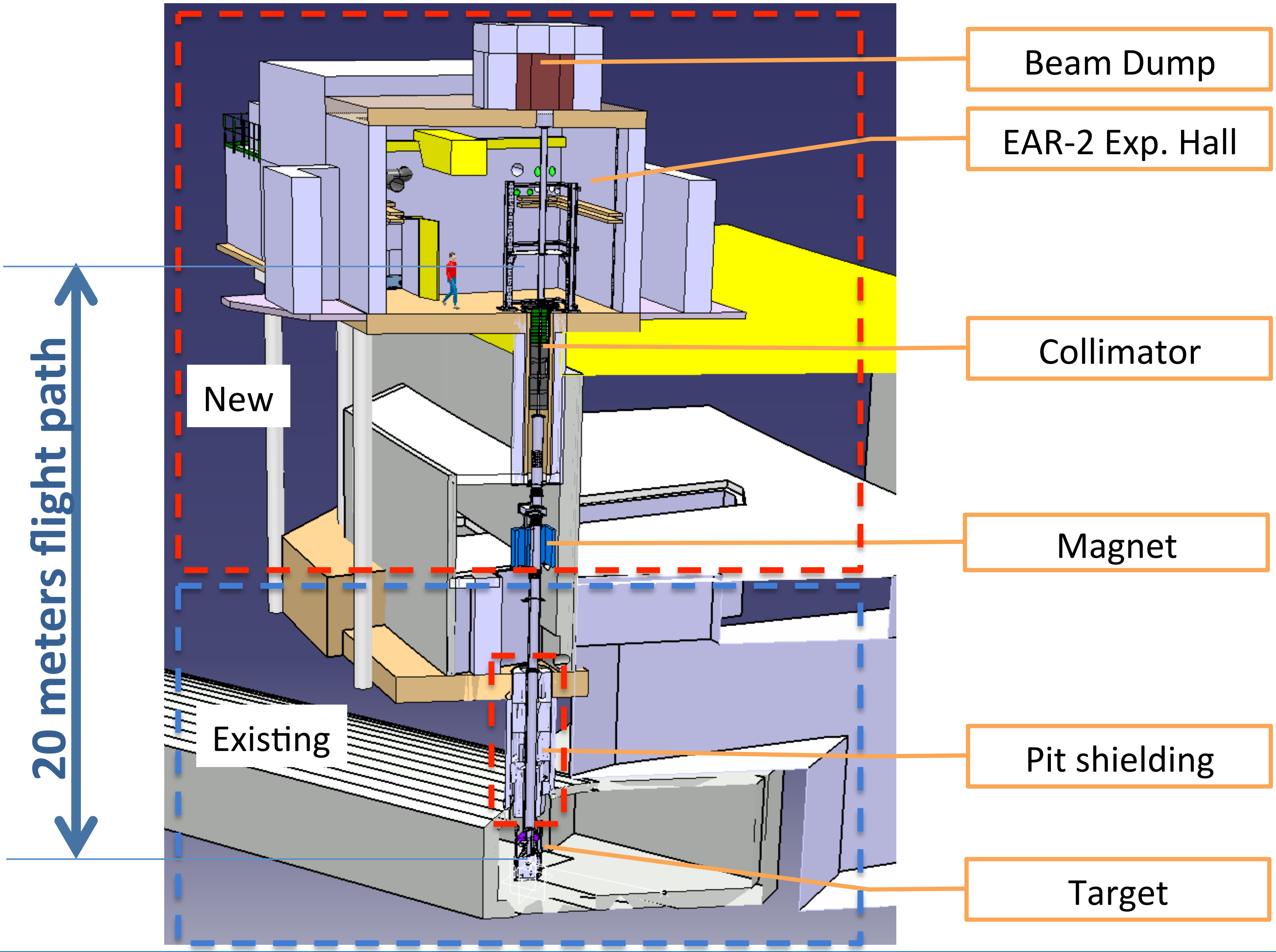

Main beam characteristics at CERN nTOF

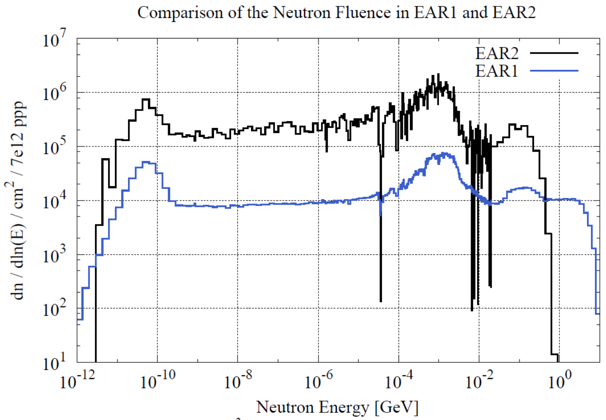

Fig. 8: *Simulated neutron fluence per cm² in the existing n_TOF experimental area (EAR-1, blue line) and in the proposed facility above the n_TOF target (EAR-2, black line). It is worth noting that, while the neutron spectrum extends up to several GeV for the EAR-1, there is a sharp cut at ~300 MeV in EAR-2.*

neutron intensity/7 10^{12} protons factor 25

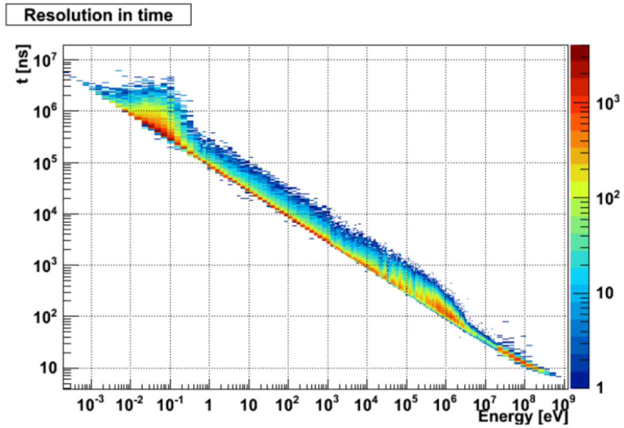

Fig. 9: *Resolution in the EAR-2, showing the relation between time of arrival and neutron energy.*

time-of-flight energy correlation

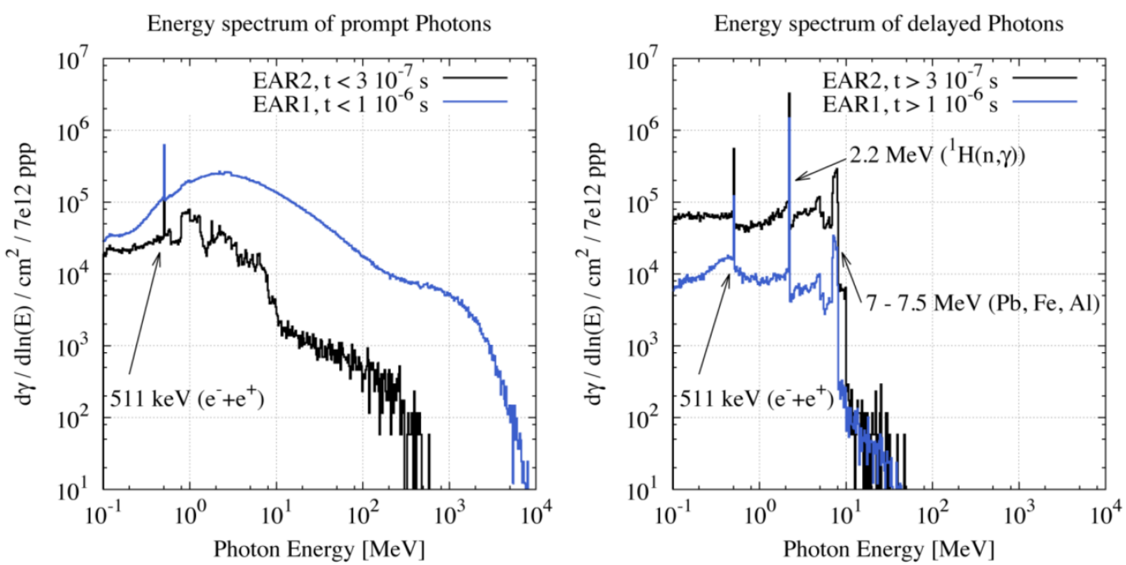

Fig. 12: *Photon energy spectrum of prompt (left) and delayed (right) photons in both facilities.*

Gammaflash reduced at EAR2

strong background from delayed photons (moderator, capture)

Detailed FLUKA simulation for the design of collimators and dump

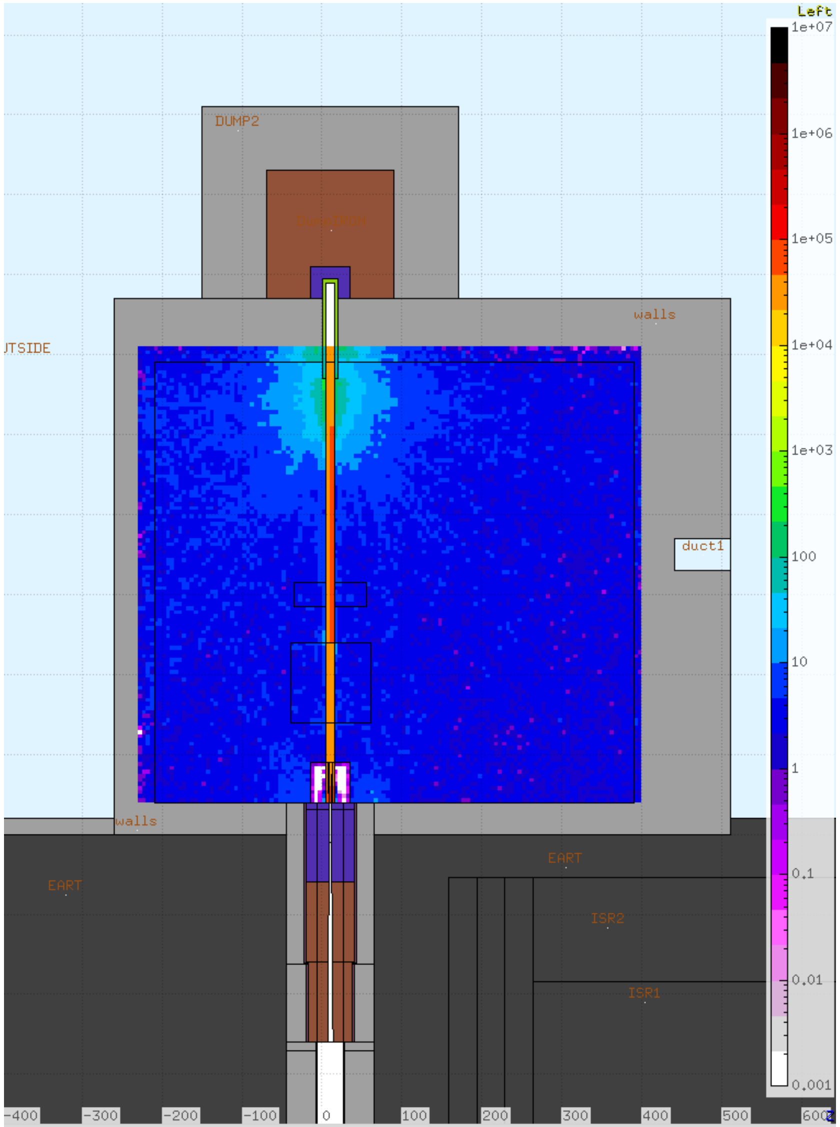

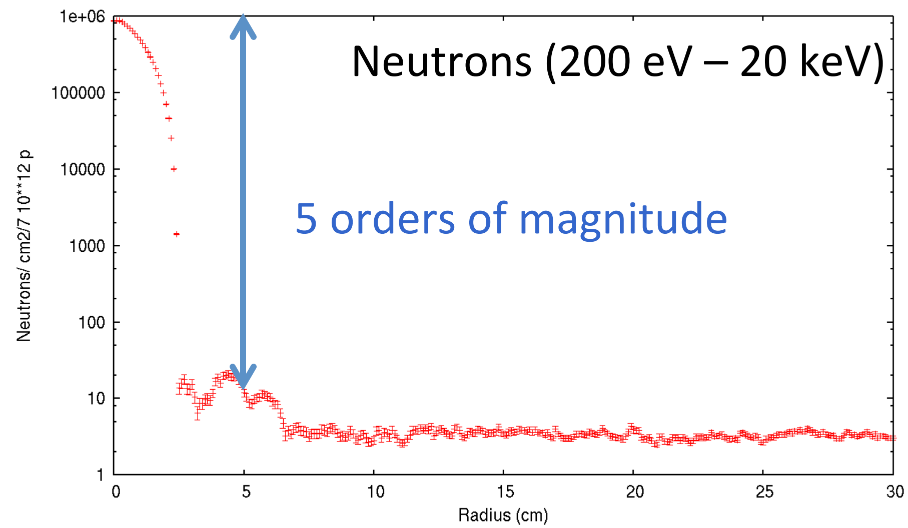

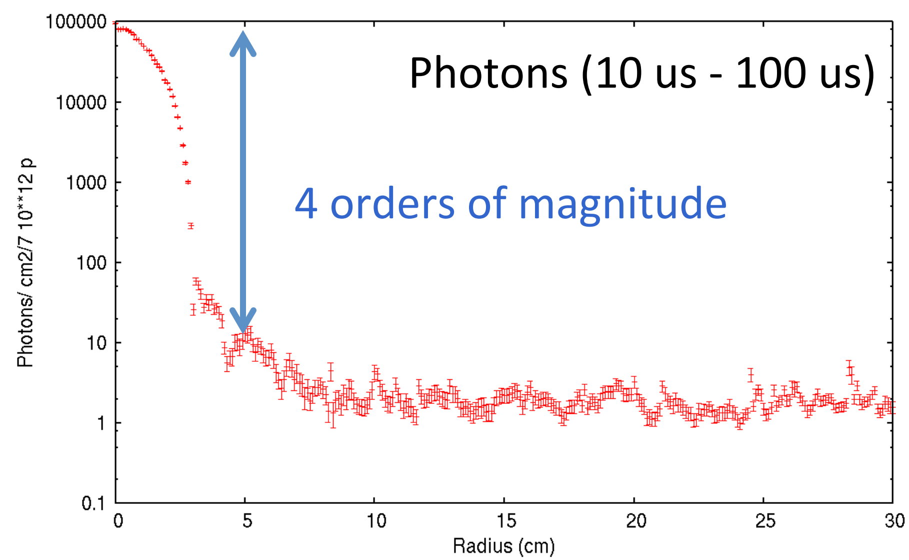

Conclusions and perspectives

The new n_TOF EAR-2 20 m neutron beam line will be operative at CERN from July 2014

25 times higher flux (n/pulse) than n_TOF EAR1 (185 m)
250 times higher flux neutron rate (n/s) than n_TOF EAR1
Reduced energy resolution(no RR above ~10 keV)
Runs in parallel to EAR1

First physics experiments by end 2014:

- Capture on fissile isotopes
- Capture on small mass *s*-process branching points
- Fission spectroscopy and prompt γ-rays with STEFF
- Elastic/inelastic reactions (HPGe or CsI+Si telescopes)
- Fission on high activity samples (e.g. ^{240}Pu)
- Irradiation of electronic components (@1.5 m)
- …

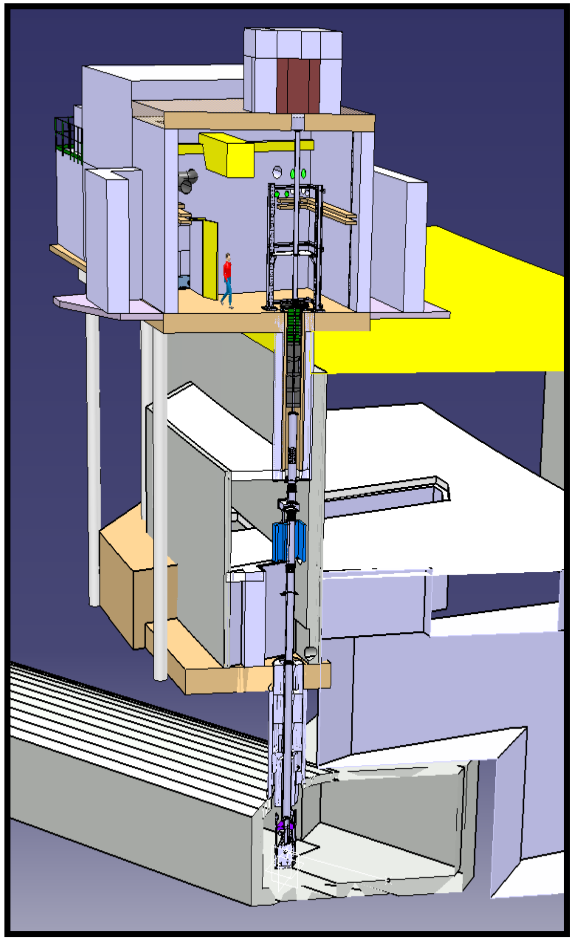

Frankfurt Neutron source in the Stern-Gerlach Center (FRANZ) $^{7}Li(p,n)^{7}Be$

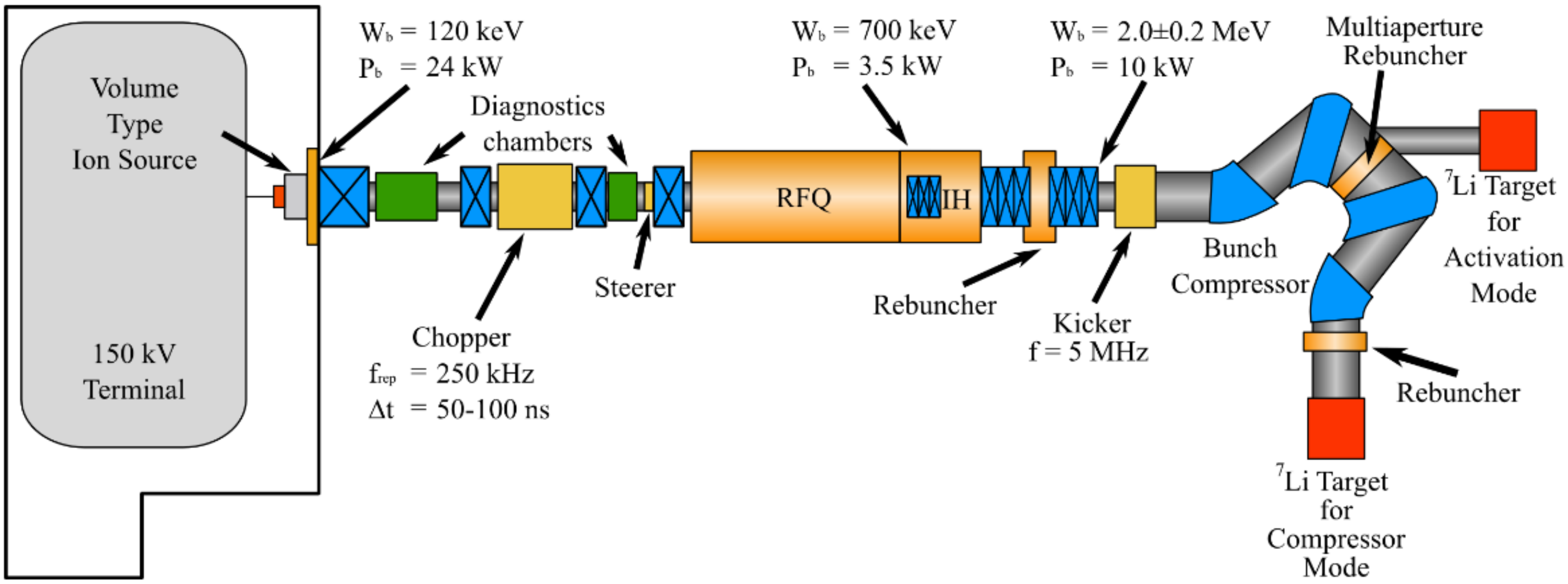

Proton accelerator: E_p = 1.8 – 2.2 MeV, 20 – 250 kHz repetition rate,
Pulse length on target: 1 ns (bunch compression)
beam power 21 kW (average beam current = 10 mA)

➔ Presentation by René Reifarth

Neutron energy: 100 – 500 keV
Neutron intensity : 5* 10^{10} n/s
on target: 3*10^{7} n/s flight path < 100 cm

Helmholtz-Zentrum Dresden-Rossendorf

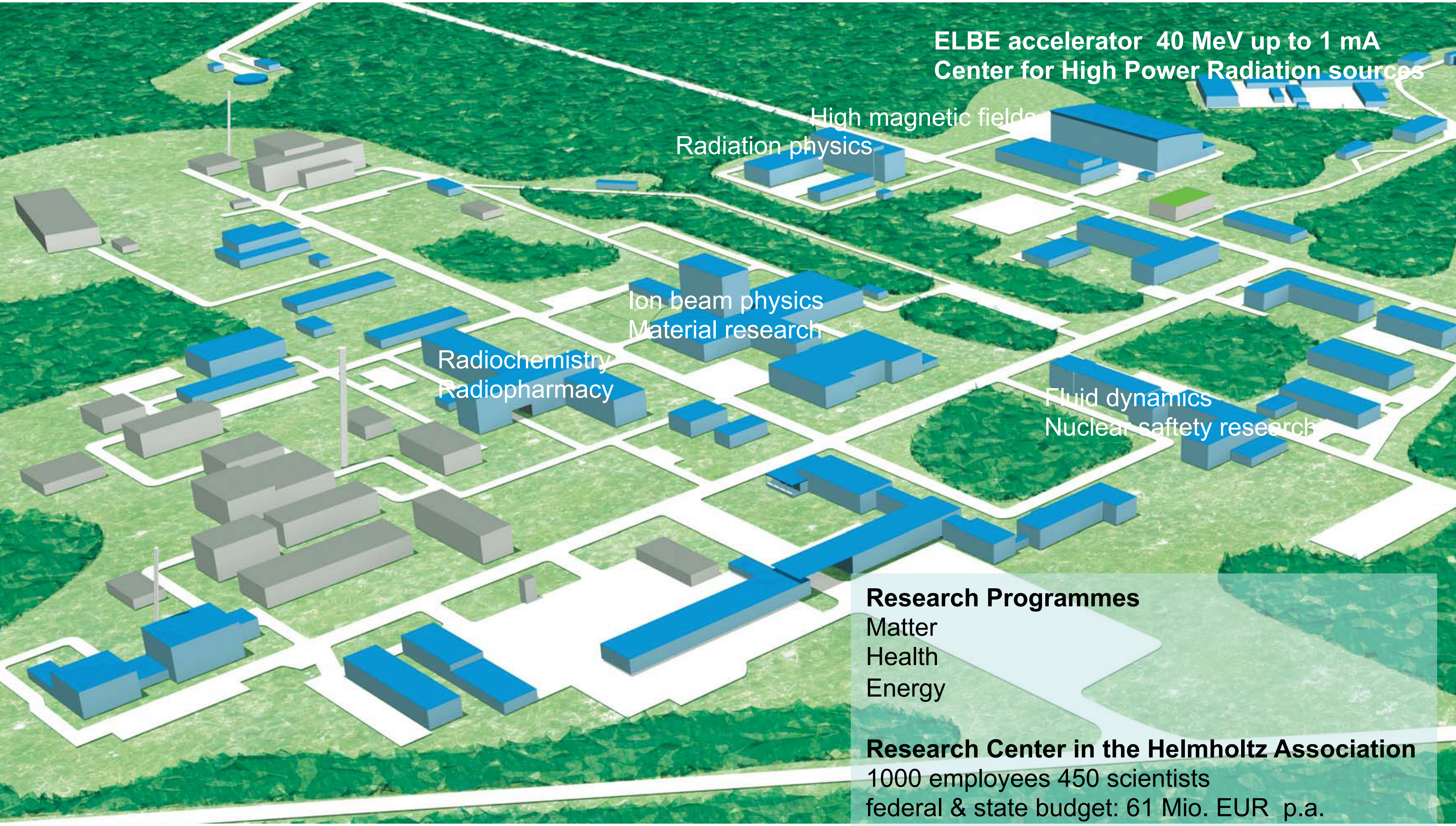

Photoneutron Source nELBE

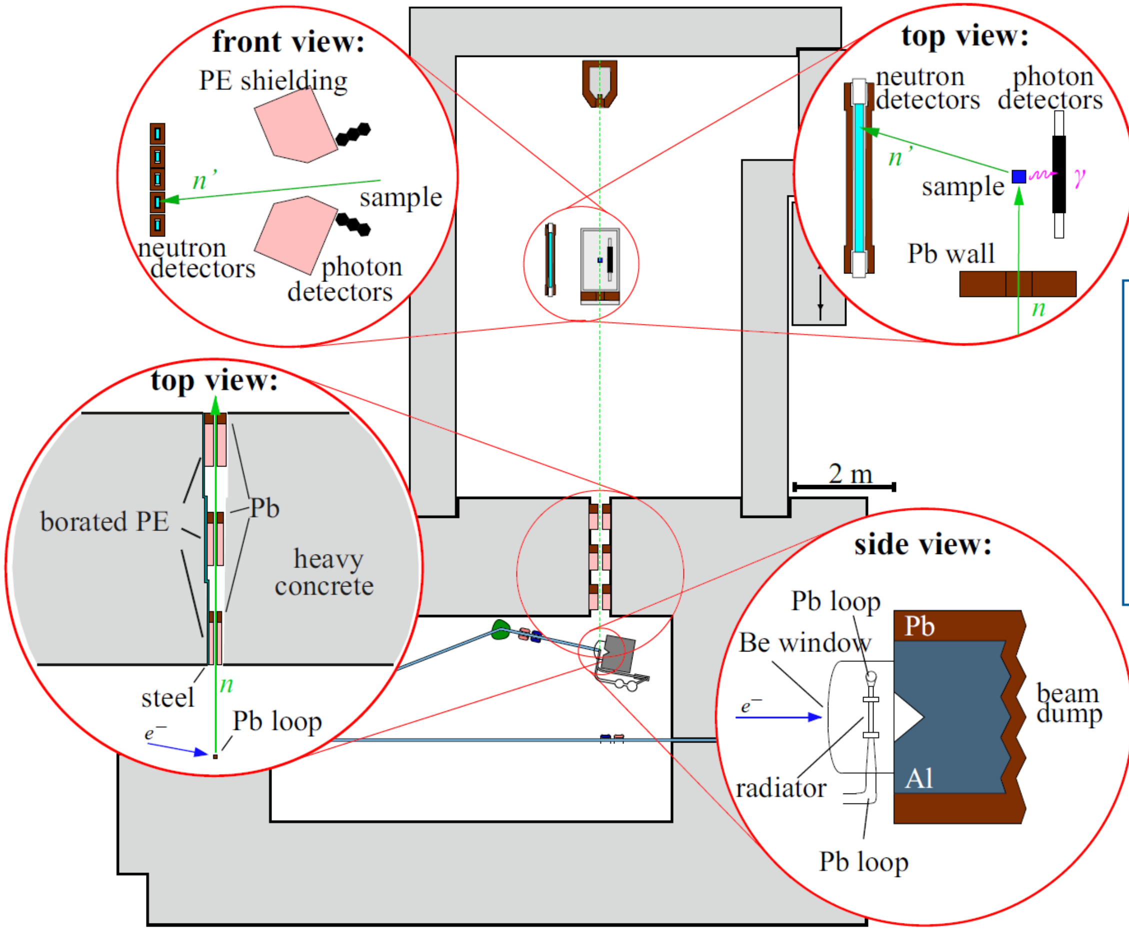

Floor plan of the new nELBE neutron source and low scattering experimental hall.

Characteristic parameters:

- repetition rate: 101 or 202 kHz
- flight path: 5 - 11 m
- source strength: ca. $1.6 \cdot 10^{11}$ n/s
- intensity @ target: ca. $2.5 \cdot 10^{4}$ n/cm^{2}s
- energy range: 10 keV - 10 MeV
- energy resolution: < 1 %

The only photo neutron source at a superconducting accelerator
New time-of-flight facility operational since August 2013.

The nELBE Neutron Time of Flight Facility
A.R. Junghans, et al.,
J. Korean Phys. Soc. **59**, 1593-1596 (2011)
Proc. Int.Conf. Nucl. Data Science and Tech, 2013 New York

DRESDEN concept HZDR

Liquid-Pb loop as neutron producing target

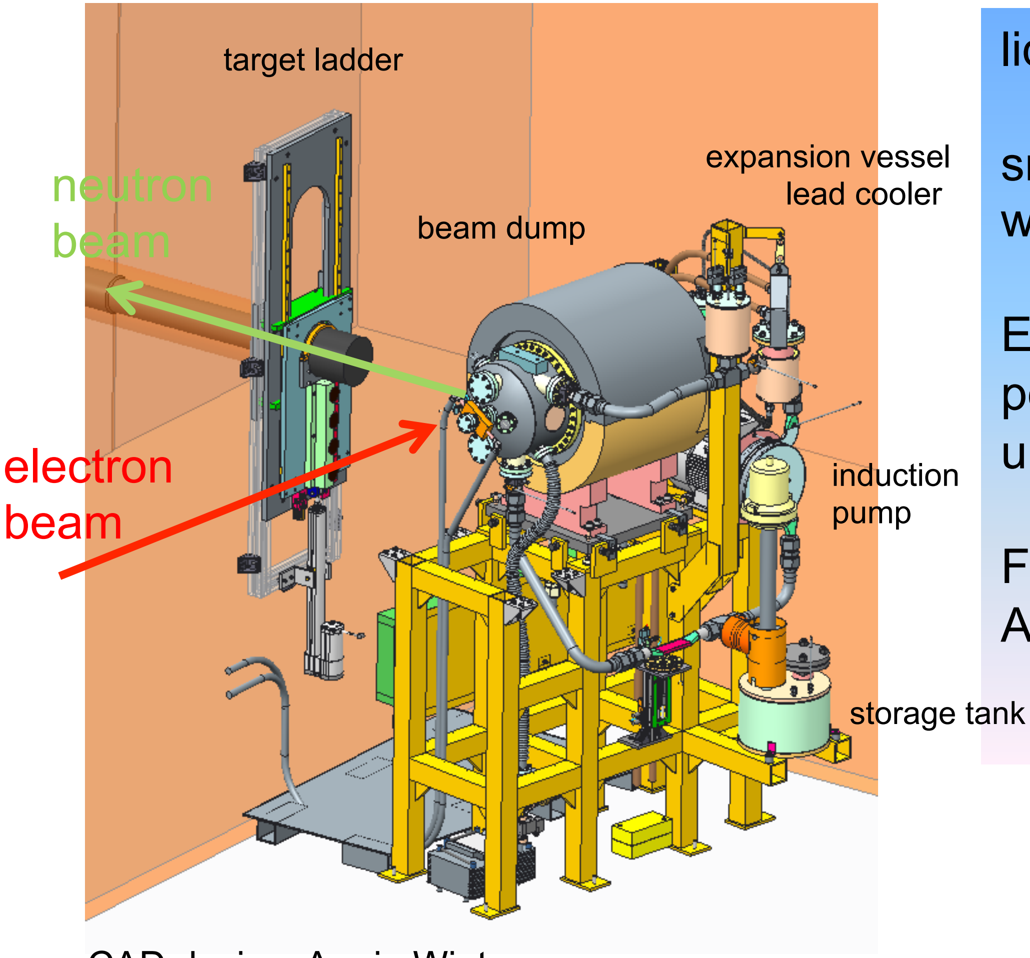

CAD design: Armin Winter

E. Altstadt et al., Ann. Nucl. Energy **34** (2007) 36

liquid lead circuit for heat transport

small Mo tube (11 mm diam.)
with liquid lead as neutron radiator

Electron beam power up to 40 kW
power density in the neutron radiator
up to 25 kW/cm^3

First beam with new Pb-loop:
August 30, 2013

DRESDEN concept HZDR

Mitglied der Helmholtz-Gemeinschaft

Photoproduction of neutrons with bremsstrahlung

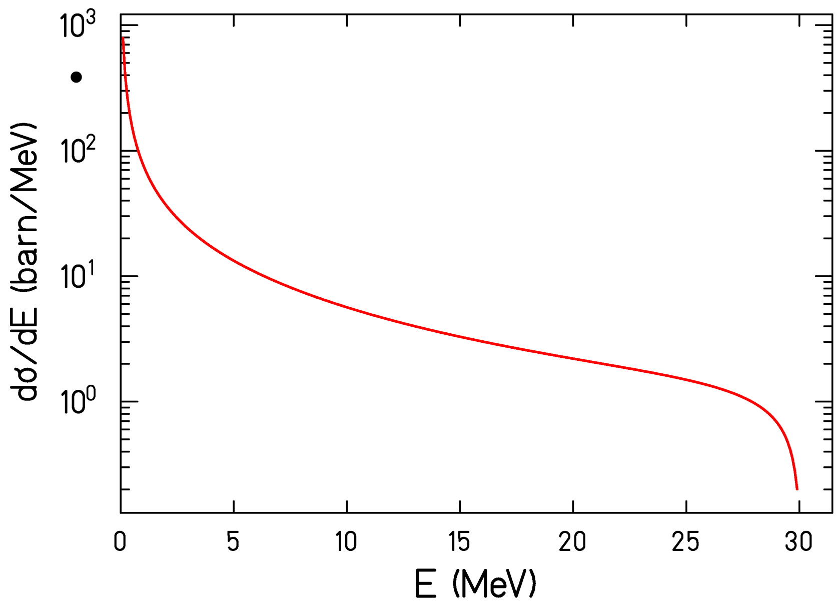

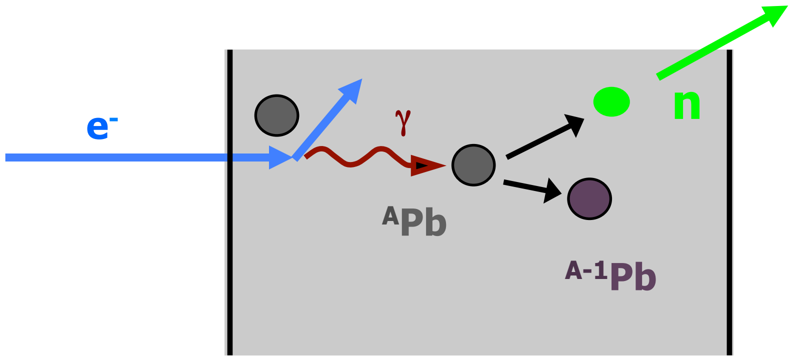

Bremsstrahlungspectrum ➔
Photonuclear excitation of
Pb through the GDR
Giant Dipole Resonance

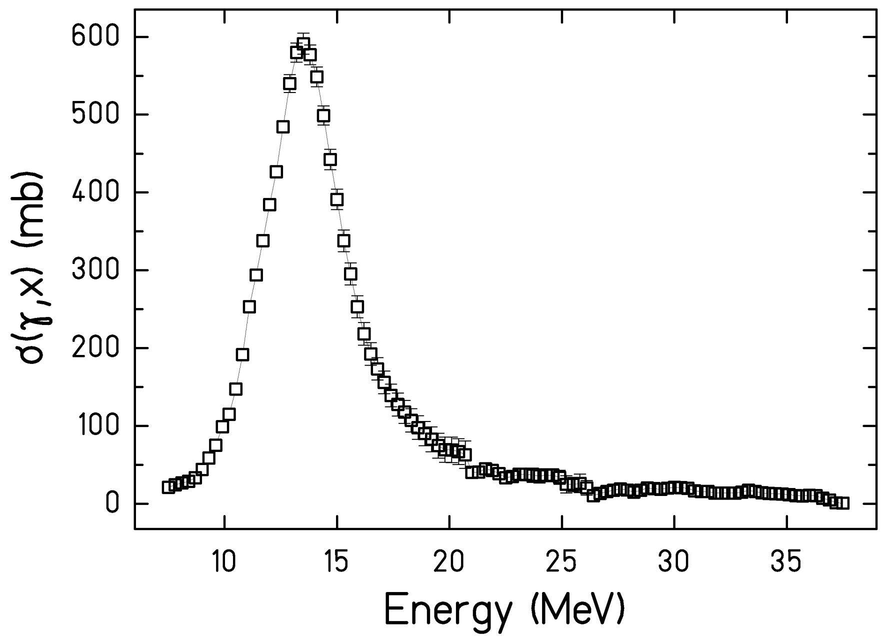

Veyssiere et al., NPA 159 (1970) 561

Neutron production by
(γ,xn) reactions

nELBE yield: $3*10^{11}$ n/s with
30 MeV 15μA (Target:Pb,liquid)
200 kHz
GELINA yield: $3*10^{13}$ n/s with
100 MeV 96μA (Target: U(Hg cooled))
800 Hz

Side remark: Normalization of photoneutron cross section measurements

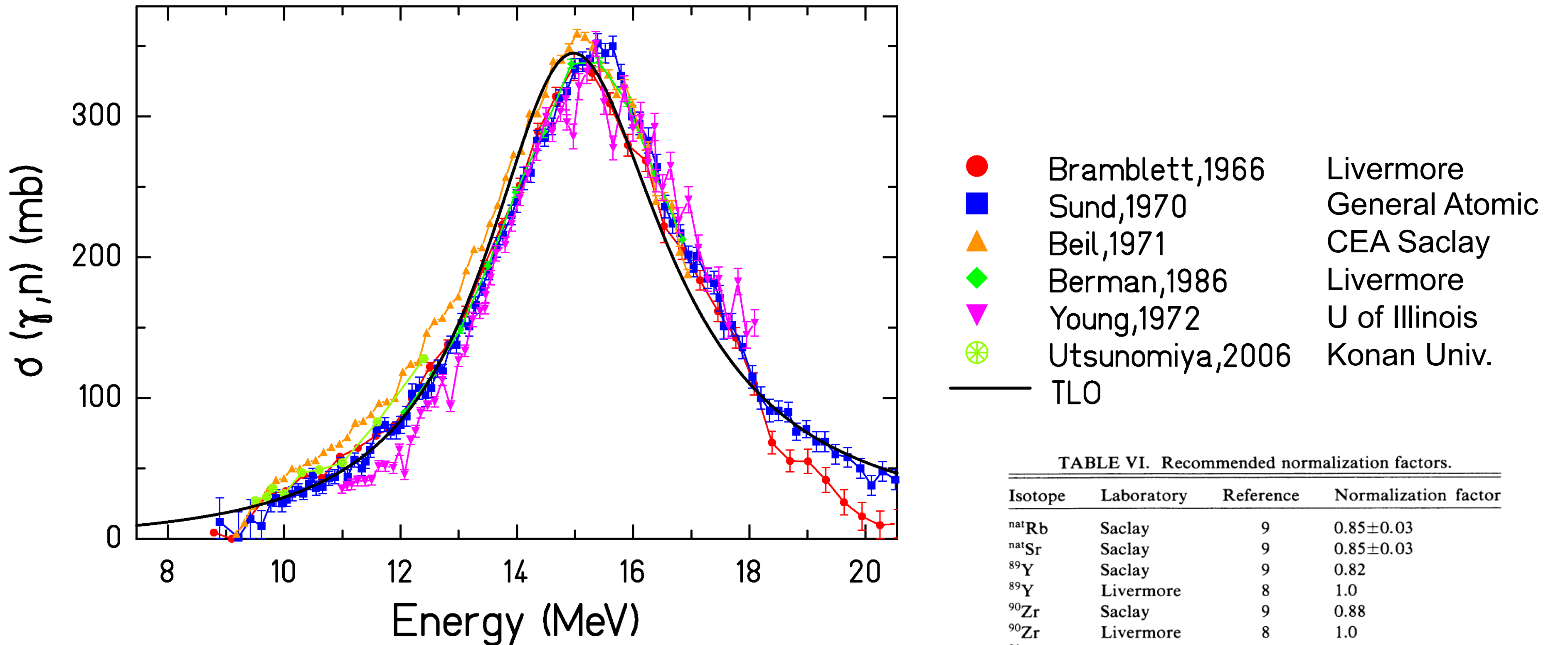

TABLE VI. Recommended normalization factors.

Isotope	Laboratory	Reference	Normalization factor
^{nat}Rb	Saclay	9	0.85±0.03
^{nat}Sr	Saclay	9	0.85±0.03
^{89}Y	Saclay	9	0.82
^{89}Y	Livermore	8	1.0
^{90}Zr	Saclay	9	0.88
^{90}Zr	Livermore	8	1.0
^{91}Zr	Livermore	8	1.0
^{92}Zr	Livermore	8	1.0
^{93}Nb	Saclay	9	0.85±0.03
^{94}Zr	Livermore	8	1.0
^{127}I	Saclay	10	0.80
^{127}I	Livermore	2	a
^{197}Au	Saclay	12	0.93
^{197}Au	Livermore	13	a
^{206}Pb	Livermore	11	1.22
^{207}Pb	Livermore	11	1.22
^{208}Pb	Livermore	11	1.22
^{208}Pb	Saclay	12	0.93
^{208}Bi	Livermore	11	1.22

[a]Do not use.

Intercalibration of different photoneutron experiments.
Berman et al. Phys. Rev. C 36 (1987) 1286
➔Renormalisation factors
This is not included in the Dietrich & Berman GDR Atlas and RIPL2/3

Nuclear reactions in the statistical model

$$W_{if} = \frac{2\pi}{\hbar}|\bar{H}_{fi}|^2 \rho_f$$
$$W_{fi} = \frac{2\pi}{\hbar}|\bar{H}_{if}|^2 \rho_i$$

Fermi's golden rule:
Averaged Matrix elements
Matrix elements have random phases because of many degrees of freedom
Averaging over $\Delta E > \Gamma$

$$\rho_c W_{c\beta} = \rho_\beta W_{\beta c}$$

for hermitian operators $|H_{if}|^2 = |H_{fi}|^2$

$$\rho_\beta = \rho_b^{frei} \cdot \rho_B(U)$$
$$\rho_b^{frei} = \frac{\tau}{2\pi^2\hbar^3} m_\beta p_\beta$$
$$p_\beta = p_b = -p_B$$
$$\frac{d\sigma}{d\Omega} = \frac{W\tau}{4\pi v_i}$$
$$\sigma = \frac{W\tau}{v_i}$$
$$\sigma_{\beta c} = \frac{W_{\beta c}\tau}{v_\beta}$$

Cross section for CN formation in channel β

$$W_{\beta c} = \frac{v_\beta \sigma_{\beta c}}{\tau}$$
$$\rho_c(E) W_{c\beta} = \frac{\tau}{2\pi^2\hbar^3} m_\beta p_\beta \rho_B(U) \frac{v_\beta \sigma_{\beta c}}{\tau}$$
$$U = E - \epsilon - S_n$$
$$\epsilon_\beta = \frac{1}{2} v_\beta p_\beta = \frac{1}{2} m_\beta v_\beta^2$$
$$W_{c\beta}(\epsilon_\beta) = \frac{\rho_B(U)}{\rho_c(E)} \frac{m_\beta \epsilon_\beta \sigma_{\beta c}(\epsilon_\beta)}{\pi^2\hbar^3}$$

Reaction rate of the CN decay in channel β as a function of kinetic energy
Depends on the ratio of the **level densities** of the **final nucleus** and the **compound system**

DRESDEN concept HZDR

Evaporation spectra from CN decay

$$\rho_c \propto \frac{1}{T} e^{E/kT}$$

$$\rho_B \propto \frac{1}{T} e^{U/kT} = \frac{1}{T} e^{(E-\epsilon-S_n)/kT}$$

$$\frac{\rho_B(U)}{\rho_c(E)} = const \cdot e^{-\epsilon/kT}$$

$$W(\epsilon_\beta) = const \cdot \sigma_{\beta c} \epsilon_\beta e^{-\epsilon/kT}$$

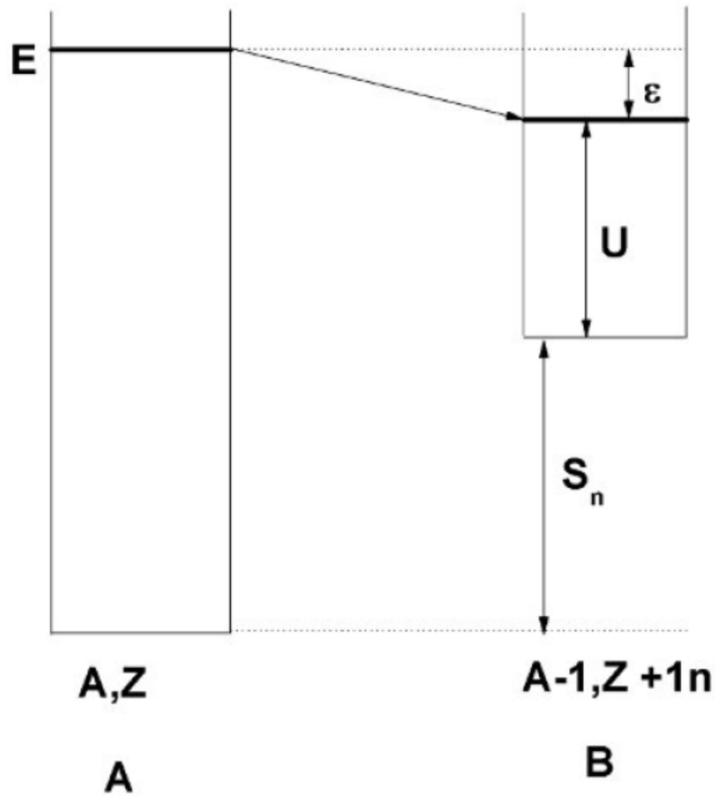

$U = E - \varepsilon - S_n$

At very large ε Transitions to Discrete excited States of the Residual nucleus B

The emission spectrum depends on:
The **level density** of the compound nucleus ρ_c
The **level density** of the residual nucleus ρ_B
And the inverse cross section of compound nucleus formation

For neutron emission $\sigma_{\beta c}$ is not strongly energy depend. ➔ Maxwellian energy spectrum
For charged particle emission: Transmission through the Coulomb-Barrier

DRESDEN concept

Neutron evaporation spectra

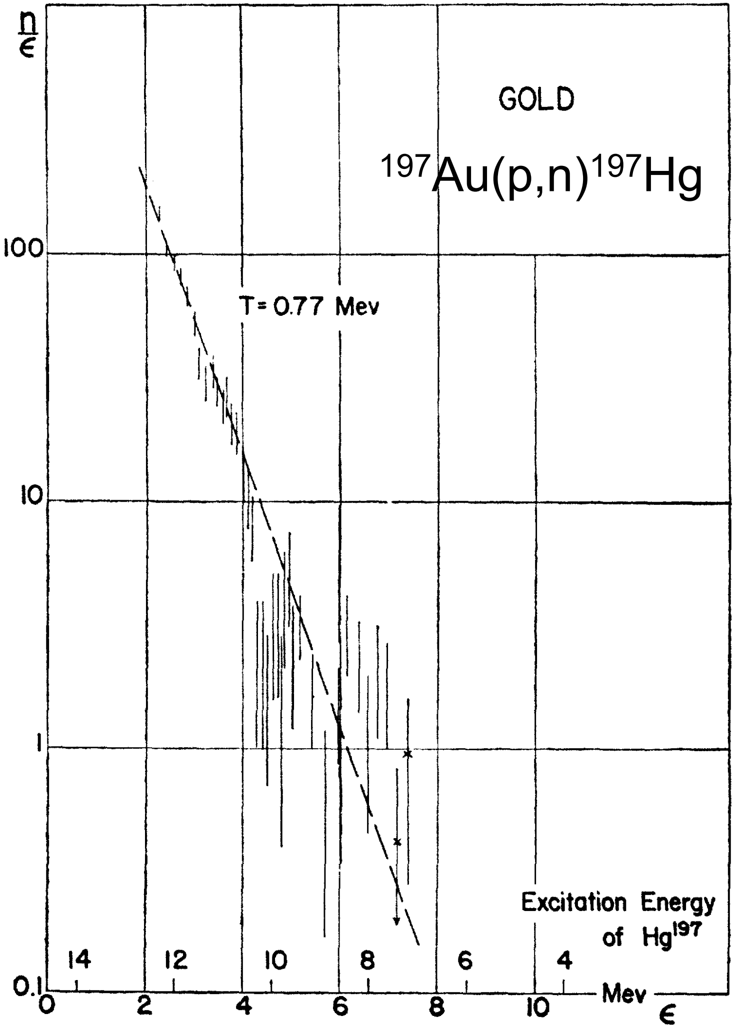

FIG. 11. Relative level density of Hg[197].

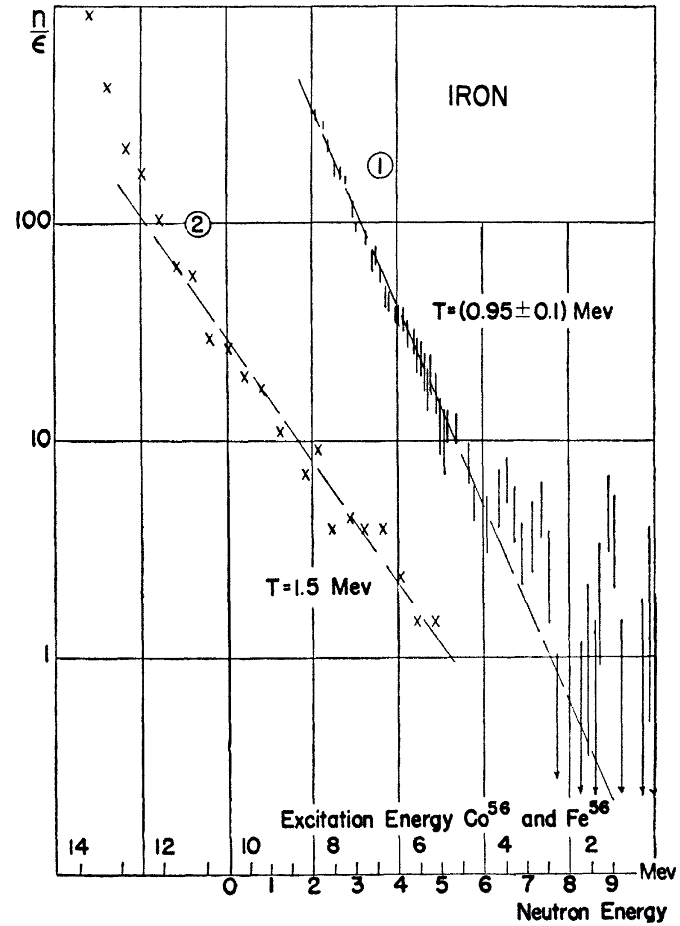

FIG. 9. Relative level density of Co^{56} and Fe^{56}. Curve 1: represents the relative level density for Co^{56} obtained from the neutron spectrum; curve 2: shows the relative level density of Fe^{56} as observed from the inelastic scattering of 16-Mev protons by iron (reference 38).

Gugelot, Phys. Rev. 81 (1951) 51

MCNP: Neutron and photon source spectra

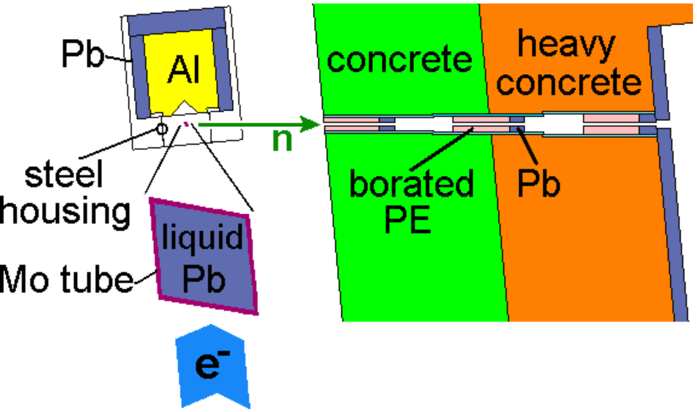

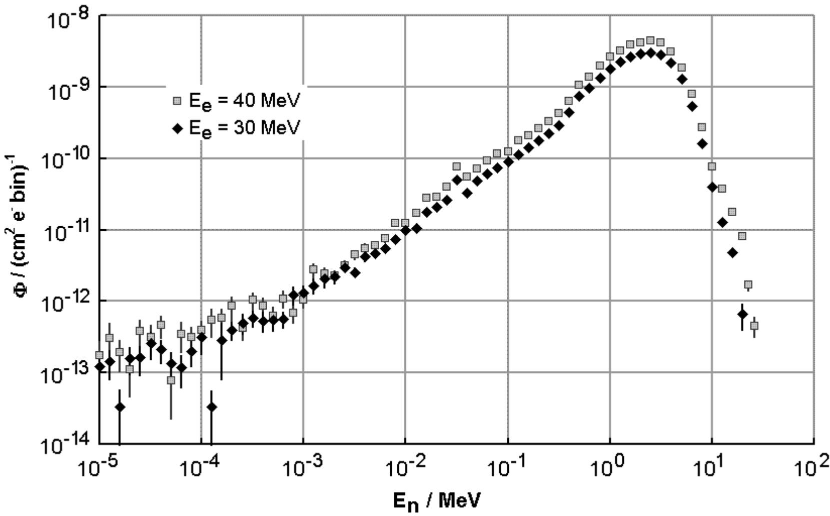

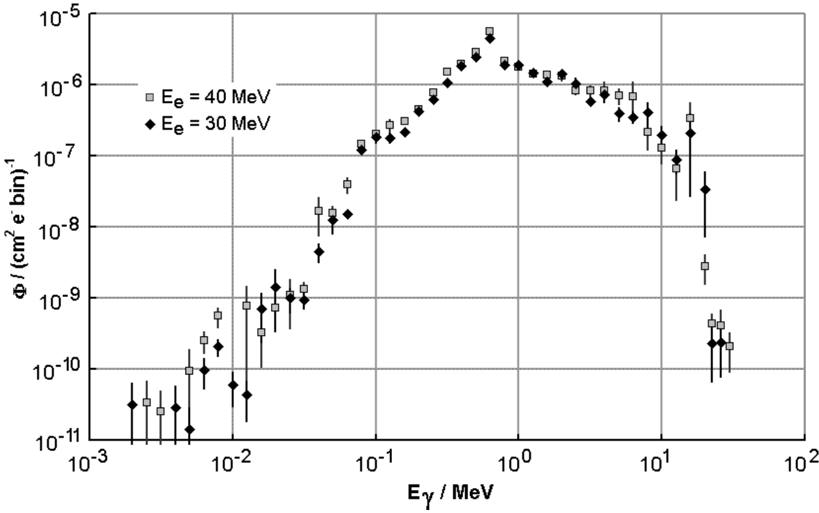

- *Mode e p n* calculation with photonuclear physics turned on
- Photonuclear cross sections for Pb and Mo adopted
- Electrons started uniformly outside Mo channel from circular disc, $\varnothing = \varnothing_{beam}$ = 8 mm
- Neutron and photon source distributions detected in collimator direction
- Distributions used as source spectra in later simulations – n & γ started uniformly from a cylindric volume (= intersection between e^- beam and Mo/Pb radiator)

➔ J. Klug et al. NIM A 577 (2007) 641

DRESDEN concept HZDR

Collimator simulation for nELBE: neutrons

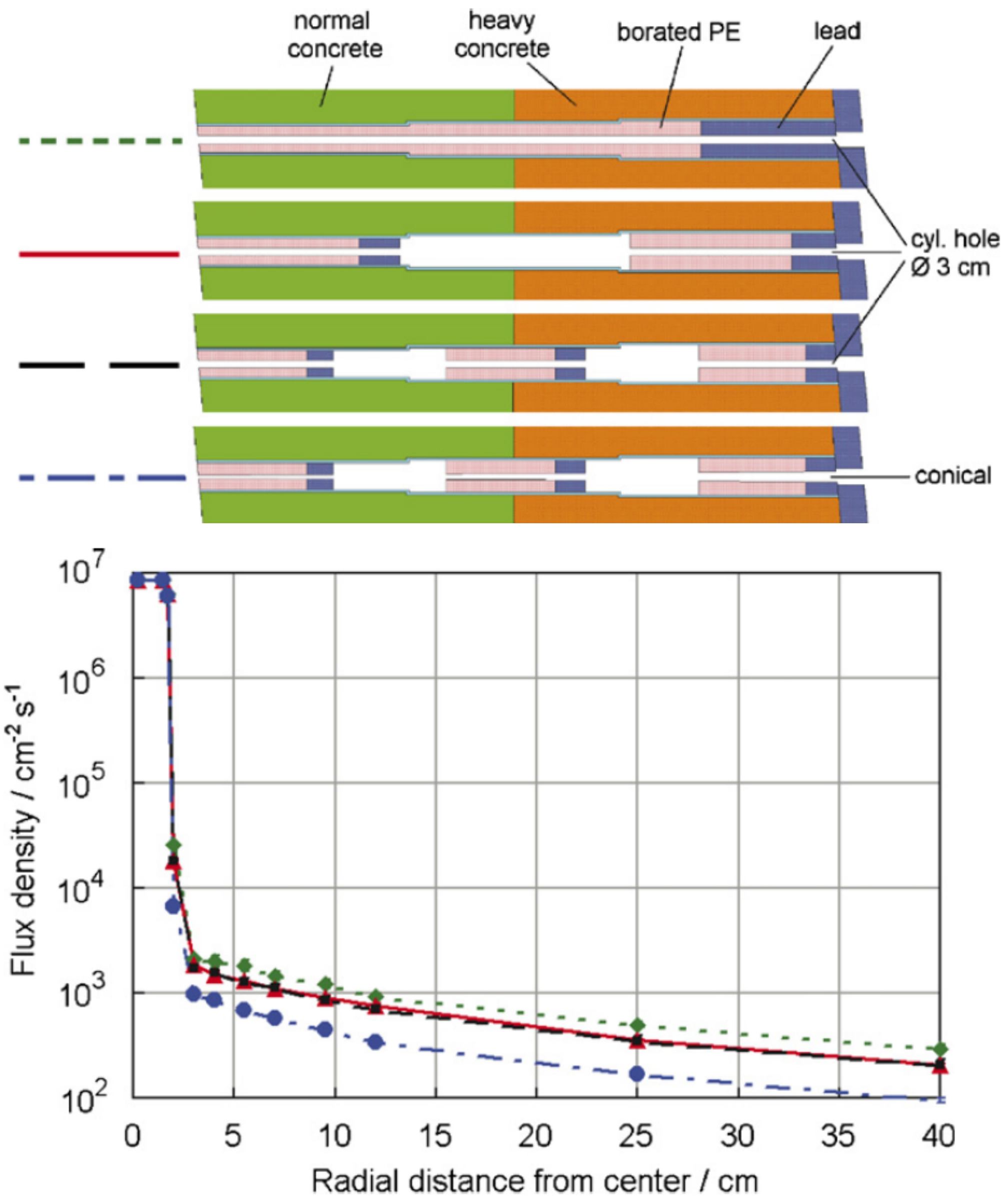

Collimator for neutrons with
Shielding capability for bremsstrahlung from the photo neutron source

Principle:
Pb for photon attenuation
borated PE for neutron attenuation

1. massive collimator has the largest beam halo
2. Two or three collimator segments do not make a big difference
3. A conical profile reduces the beam Halo compared with a cylindrical profile

J. Klug et al. NIM A 577 (2007) 641

Collimator simulation for nELBE: bremsstrahlung

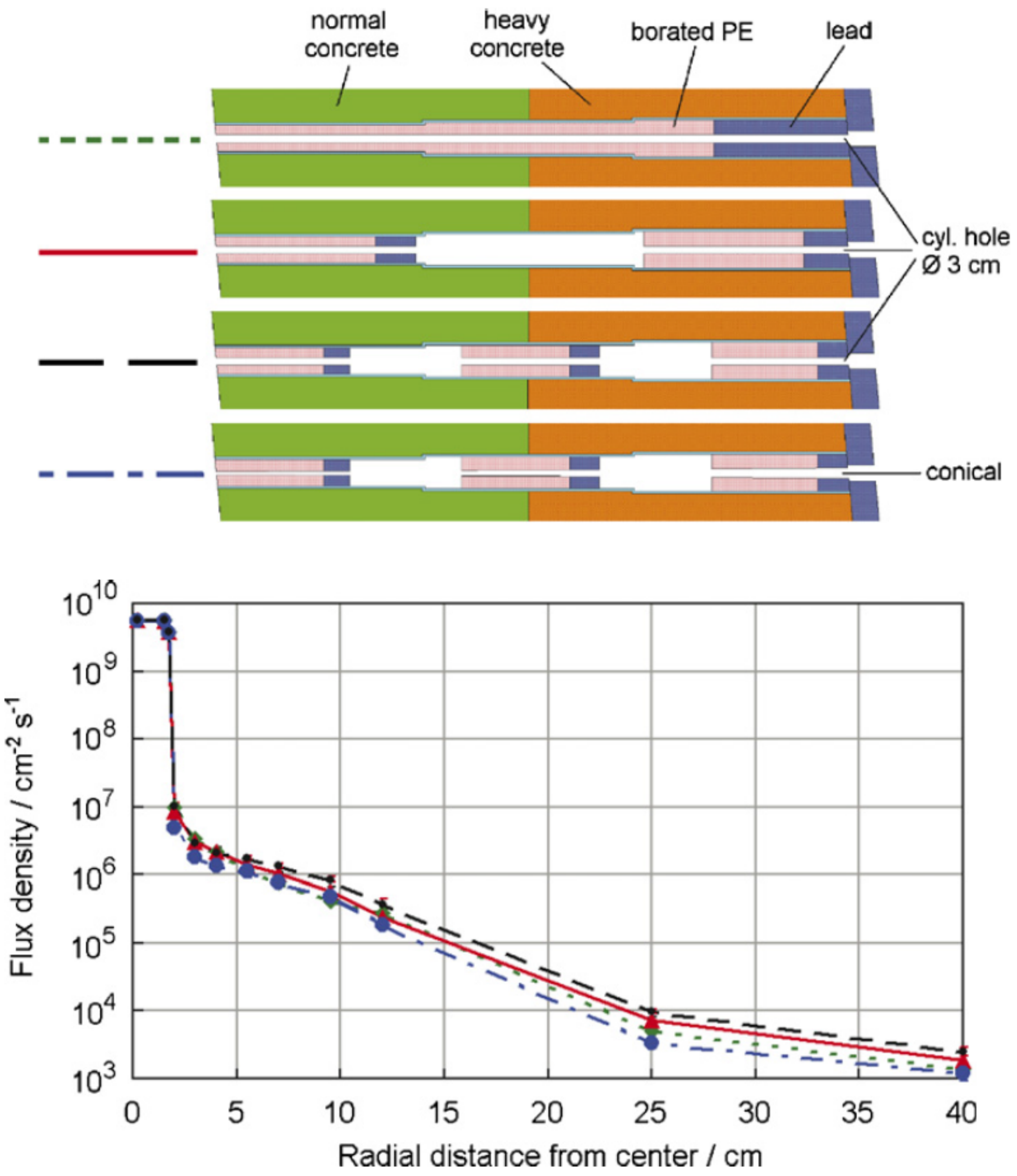

Collimator for neutrons with Shielding capability for bremsstrahlung from the photo neutron source

Principle:
Pb for photon attenuation
borated PE for neutron attenuation

1. Photon halo is much wider than the neutron halo
2. Three segments seem to be a little better than two segments
3. A conical profile reduces the beam halo compared with a cylindrical profile

Measured beam profile at nELBE

R. Beyer et al. / Nuclear Instruments and Methods in Physics Research A 723 (2013) 151–162

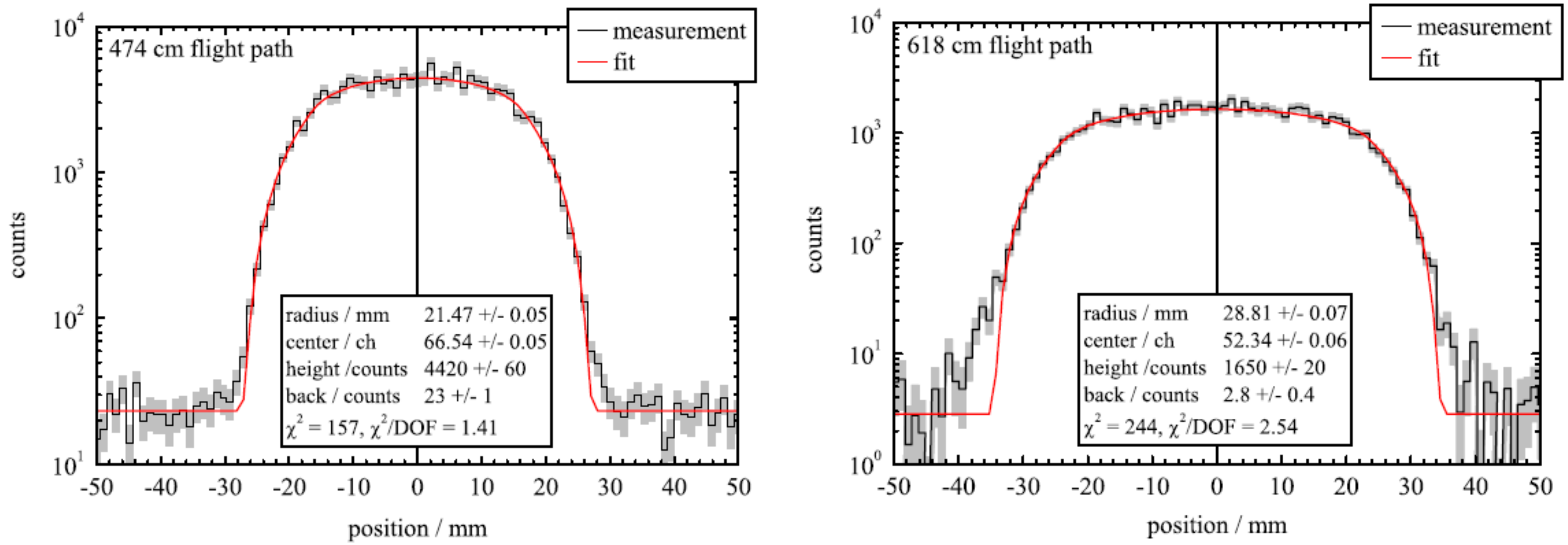

Beam profile from a one dimensional scan with a bar shaped scintillator
By time-of-flight only the neutron component is measured.
Reduction of the count rate in the beam halo by a factor 1.7 10^{-3}

The fitted curve assumes perfect rectangular beam profile with no halo.
The measurement position is farther away from the collimator exit.
Additional scattering by layers of matter in the beam (air, fission chamber)

Time of flight spectrum

dead-time corrected count rate with ^{197}Au sample (red) and fitted background (blue)

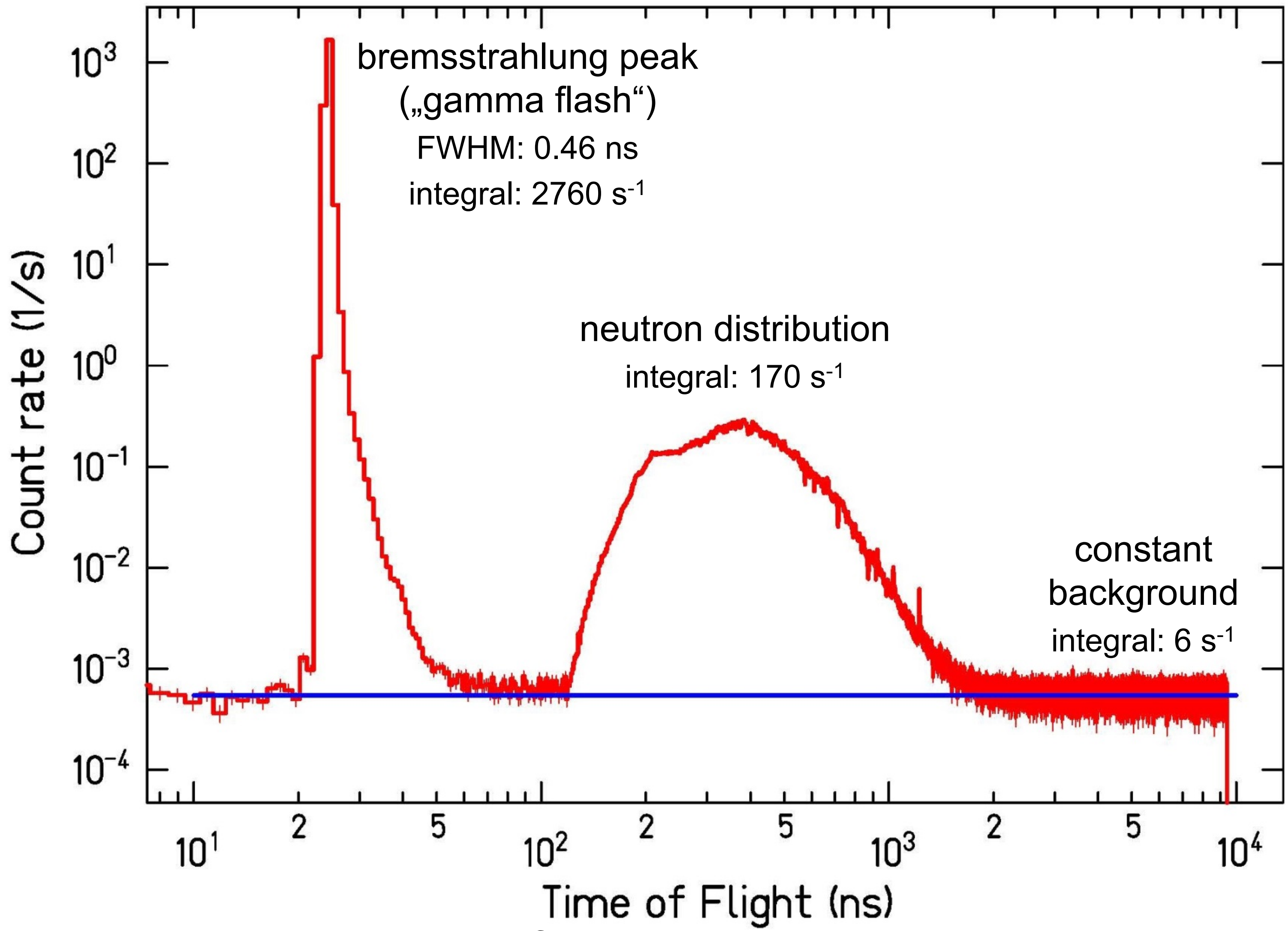

neutron intensity strongly reduced for transmission measurement
detection threshold ca. 5 keV

nELBE time of flight spectrum

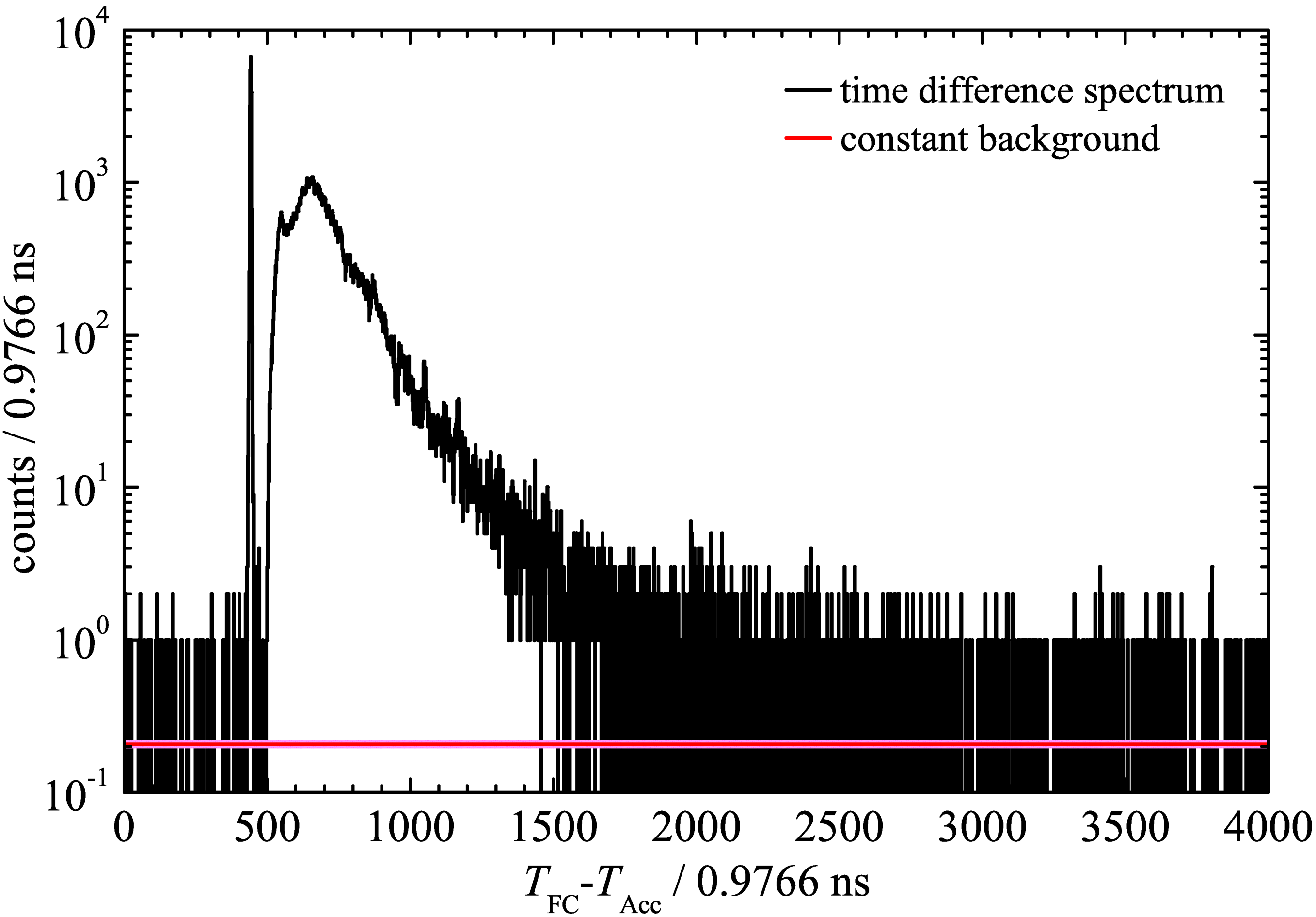

^{235}U fission chamber H19 from PTB.

Bremsstrahlung-induced fission is visible.

Time resolution from peak width = 3.8 ns FWHM

DRESDEN concept

HZDR

nELBE neutron spectrum

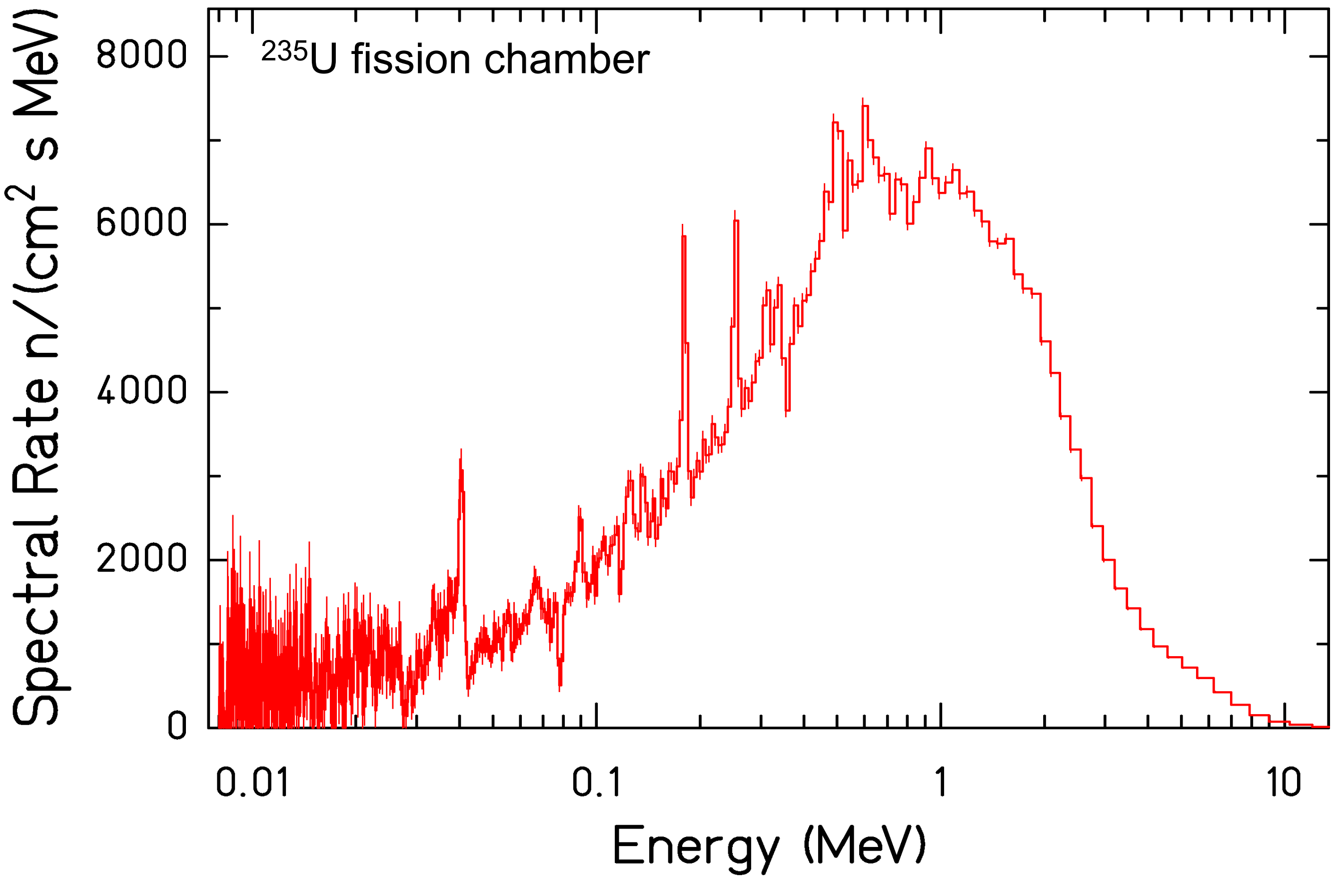

Measurement time : 49.4 h I_{e-} = 15 µA, E_{e-} = 31 MeV
Flight path 618 cm
Absorption dips : 78,117, 355, 528, 722, 820 keV ^{208}Pb scatttering resonances
Emission peaks: 40,89,179, 254, 314, 605 keV near threshold photoneutron emission
In ^{208}Pb (strong capture resonances of ^{207}Pb)

R. Beyer et al., NIM A723 (2013) 151

GELINA pulsed neutron source

Electron accelerator

- 150 MeV electron accelerator
- 10 ns burst, 10 A peak
- 800 bursts/s

Compression magnet

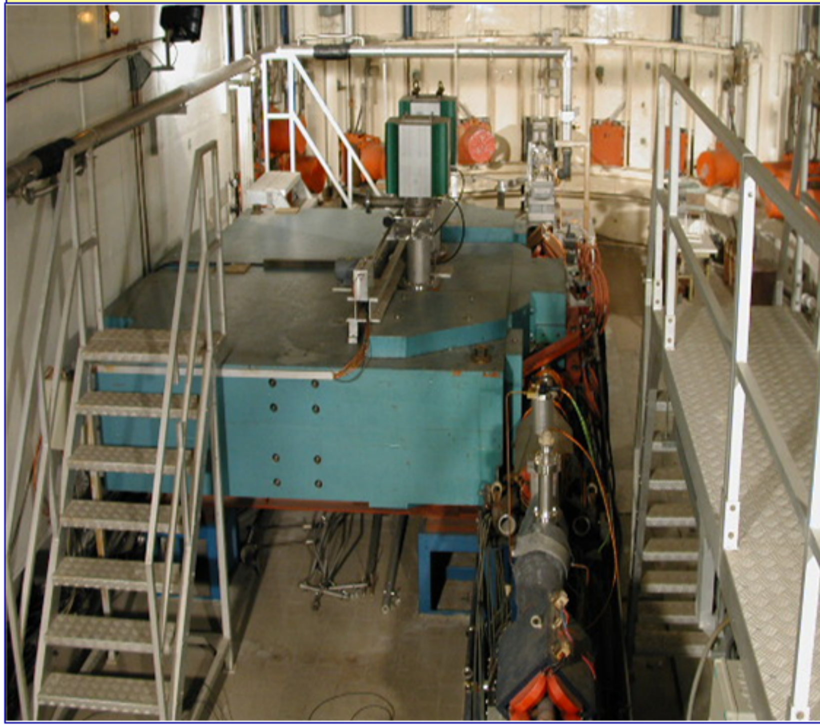

- Pulse compression magnet
- <1 ns burst, >100 A peak

Electron-neutron conversion target

- Uranium target – rotating, mercury cooled
- 4 10^{10} neutrons / burst

water-filled Be moderators

12 Flight paths
8 to 400 m

moderated or fast neutron spectrum
24 h/d, 100 h/w

GELINA target moderator / tof dependent background

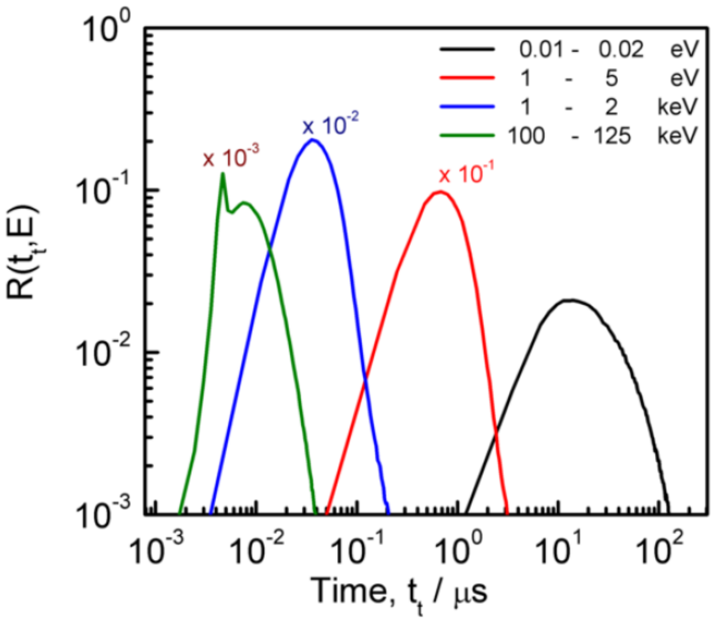

FIG. 1. The probability distribution of the time t_t that a neutron spends in the target-moderator assembly of GELINA.

slowing down time longer for lower neutron energy

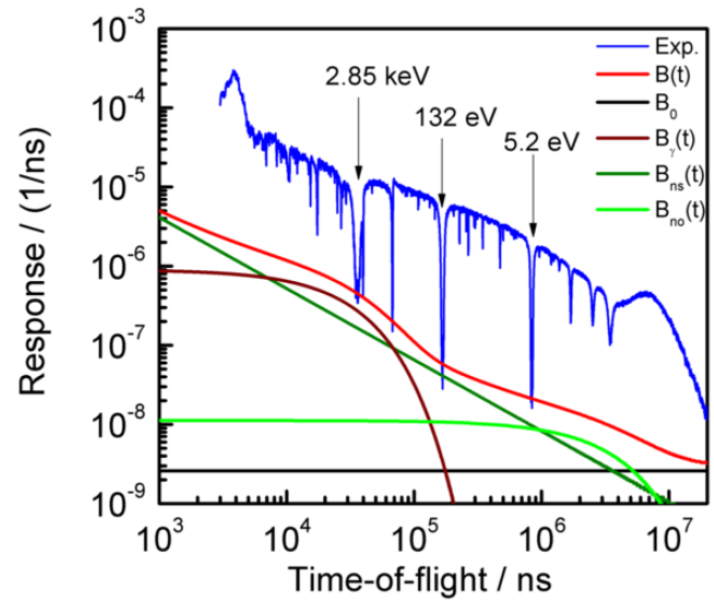

FIG. 11. The response of a Li-glass detector as a function of TOF for measurements at GELINA, is shown together with the total background and the contribution of the different components. The response is the result of a sample-in measurement on ^{241}Am [69].

tof dependent background:
capture γ rays in hydrogen moderator
overlap neutron, scattered neutrons and neutrons from adjacent beamlines

Schillebeeckx et al. NDS 113 (2012) 3054

GELINA neutron spectrum and energy resolution

Flaska et al., NIM A531 (2004) 394

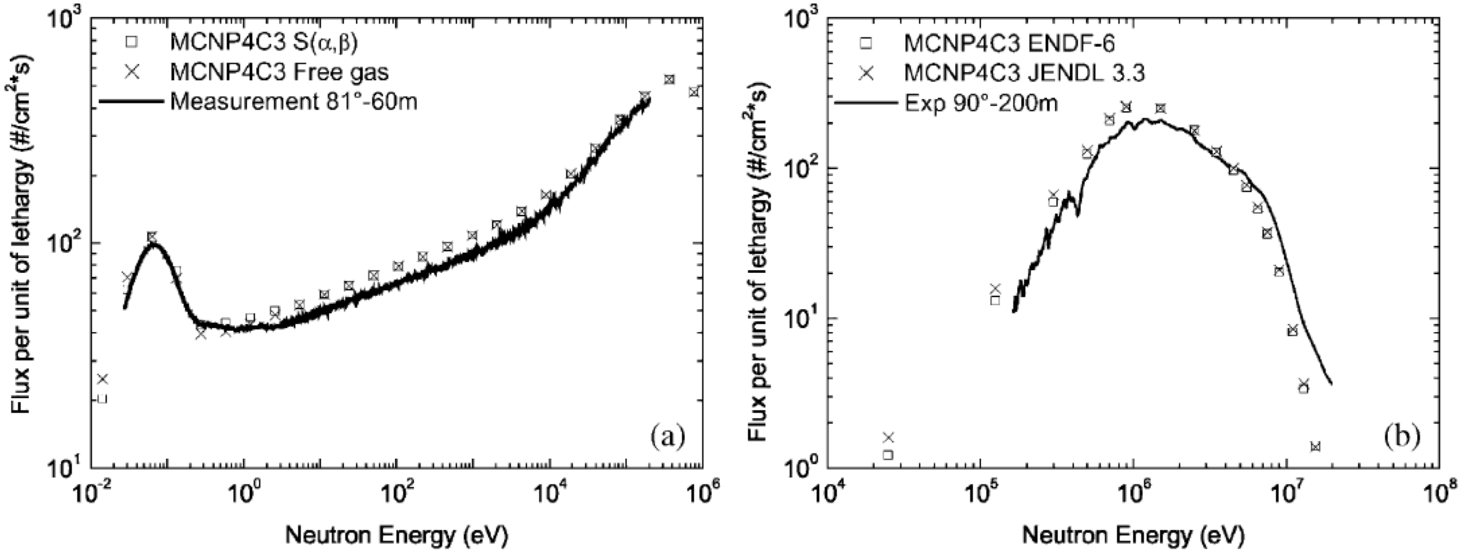

Fig. 4. Neutron flux per unit of lethargy in the flight-path. (a) 81°—60 m of the moderated neutron spectrum; (b) 90°—200 m of the fast neutron spectrum.

Schillebeeckx et al. NDS 113 (2012) 3054

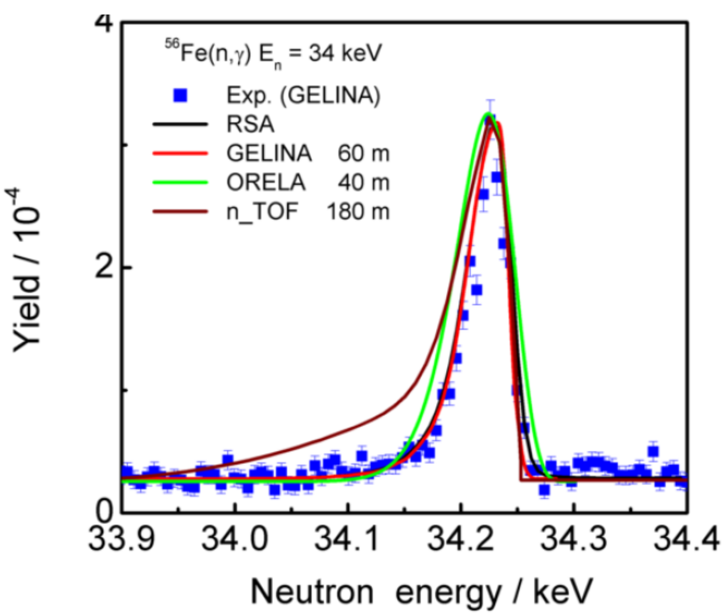

Fast neutron spectrum from 0.1 – 18 MeV

GELINA:

- width is dominated by the tof-resolution
  resonance total $\Gamma \approx$ 2 eV
  Doppler width (FWHM) ≈ 13 eV
  ToF resolution (FWHM) ≈ 40 eV
- photoneutron sources tend to have a higher resolution than spallation neutron sources (larger target-moderators required)

The Neutrons For Science facility at SPIRAL-2

X. Ledoux and the NFS collaboration

Description

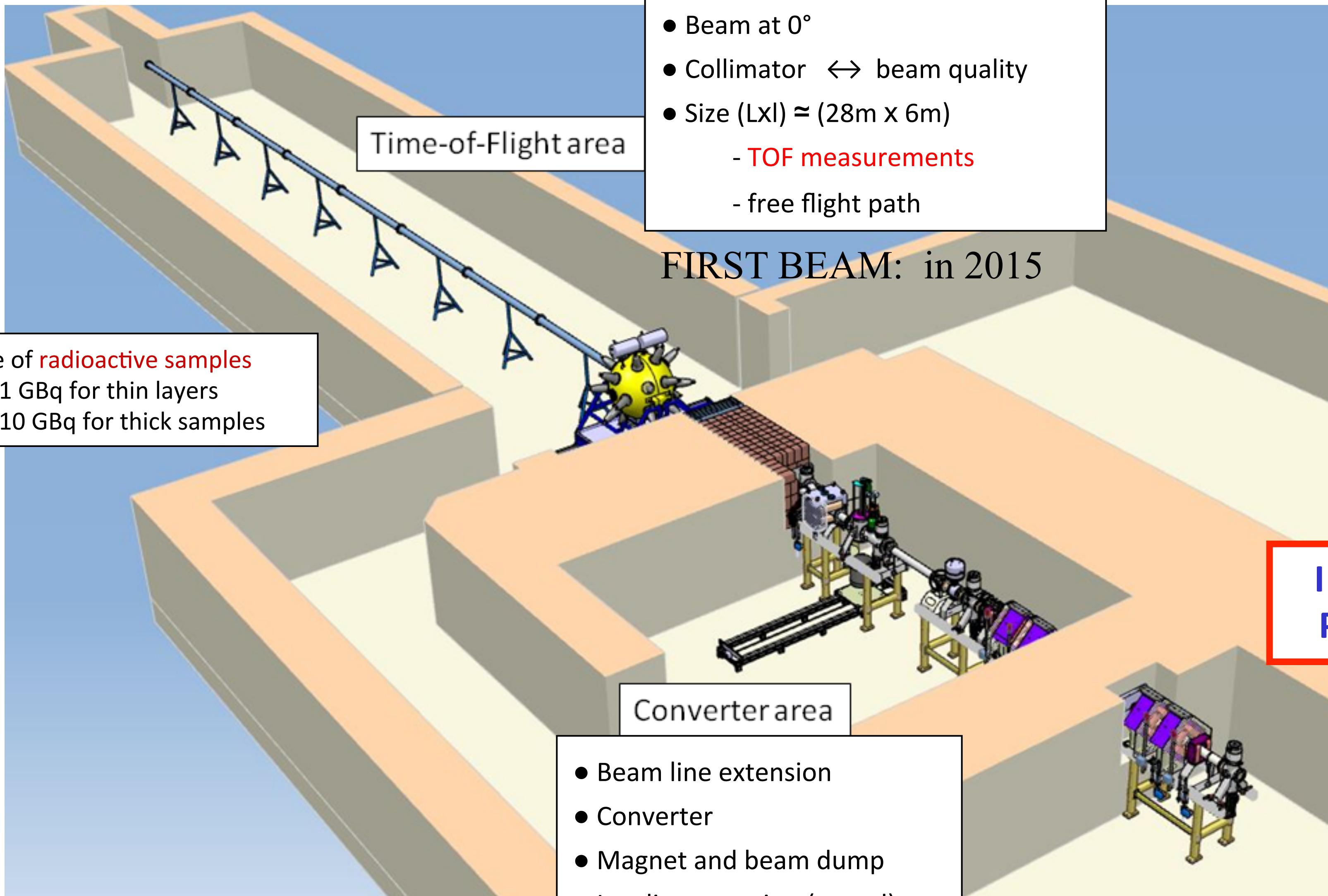

- Beam at 0°
- Collimator ↔ beam quality
- Size (Lxl) ≈ (28m x 6m)
  - TOF measurements
  - free flight path

FIRST BEAM: in 2015

Use of radioactive samples
A< 1 GBq for thin layers
A< 10 GBq for thick samples

I < 50 μA
P < 2 kW

- Beam line extension
- Converter
- Magnet and beam dump
- Irradiaton station (n, p, d)

Neutron spectra provided at NFS

Characteristics of the beams the LINAG :

- 40 MeV deuteron and 33 MeV proton
- I_{max} = 5 mA
- Pulsed beam F_0 = 88 MHz T=11 ns Burst width = 200 ps

Continuous spectrum :

E_{max} = 40 MeV , <E> = 14 MeV

thick converter (1cm)

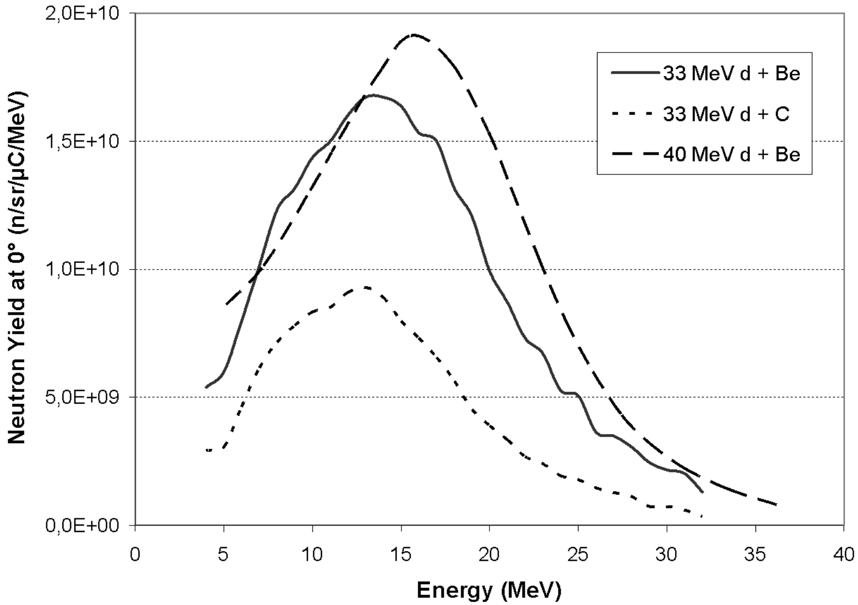

J. P. Meulders et al., Phys. Med. Biol. (1975)vol 20 n°2, p235

M. J. Saltmarsh et al., NIMA145 (1977) p81-90

Quasi-monokinetic beam :

E_n = up to 31 MeV

Thin converter (1-3 mm)

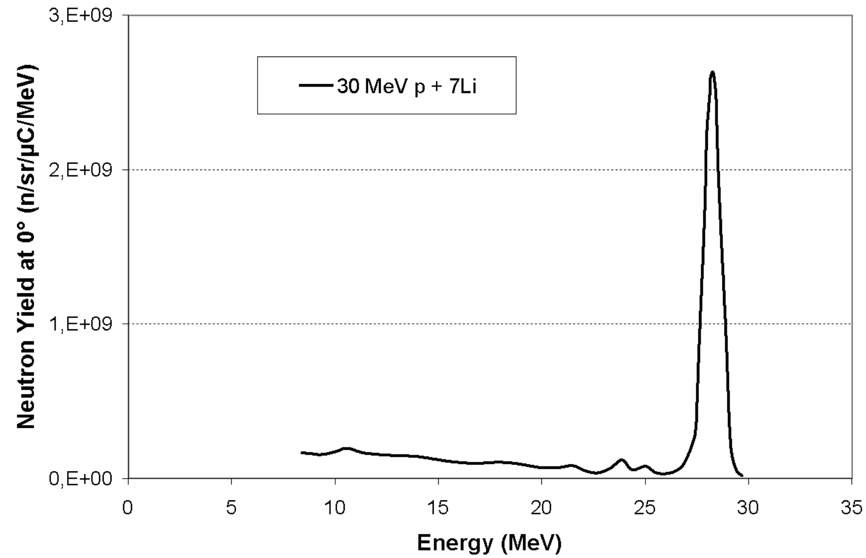

C. J. Batty et al.,NIM **68** (1969) p273-276

⇒ Similar to IFMIF spectrum

Single bunch selector for time-of-flight measurements:
Repetition rate: 150 kHz – 1 MHz

Neutron flux in the TOF area

NFS : 40 MeV d + Be

WNR : Los Alamos

n-TOF 2 : CERN

n-TOF 1 : CERN

GELINA : Geel

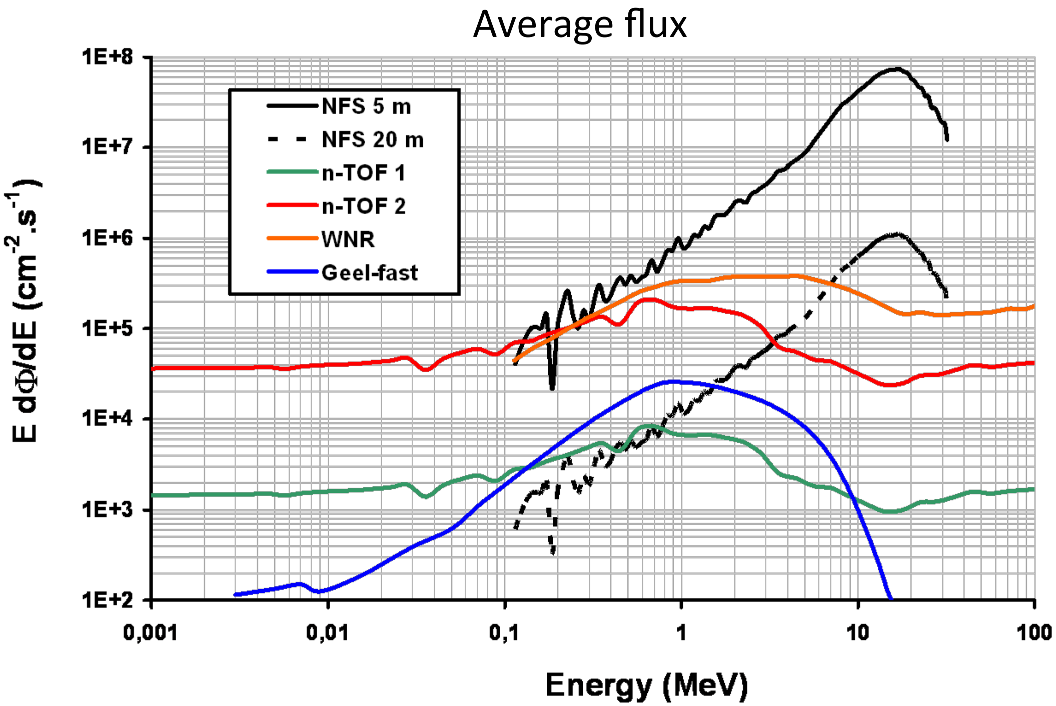

- E_n: from 0,1 MeV to 40 MeV
- Good energy resolution
- Reduced γ flash
- Low instantaneous flux

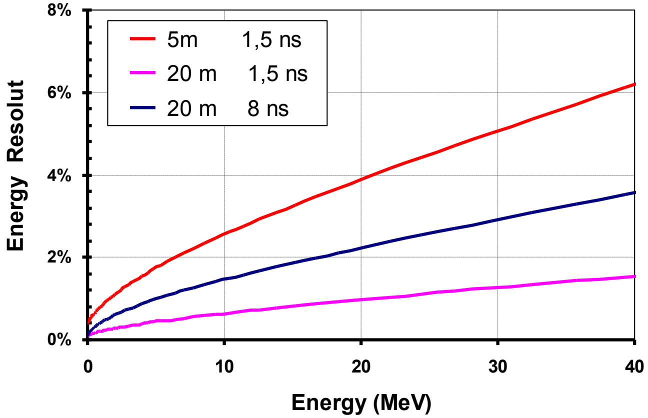

→ Complementary to the existing facilities

Research Reactor: Heinz Maier-Leibnitz FRM-II Garching

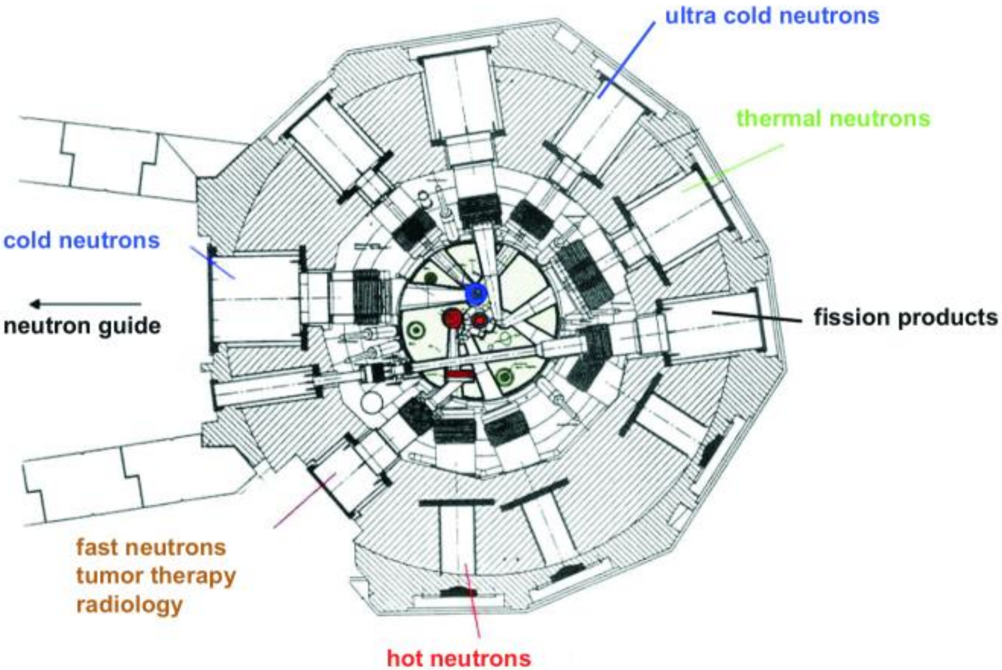

http://www.frm2.tum.de/

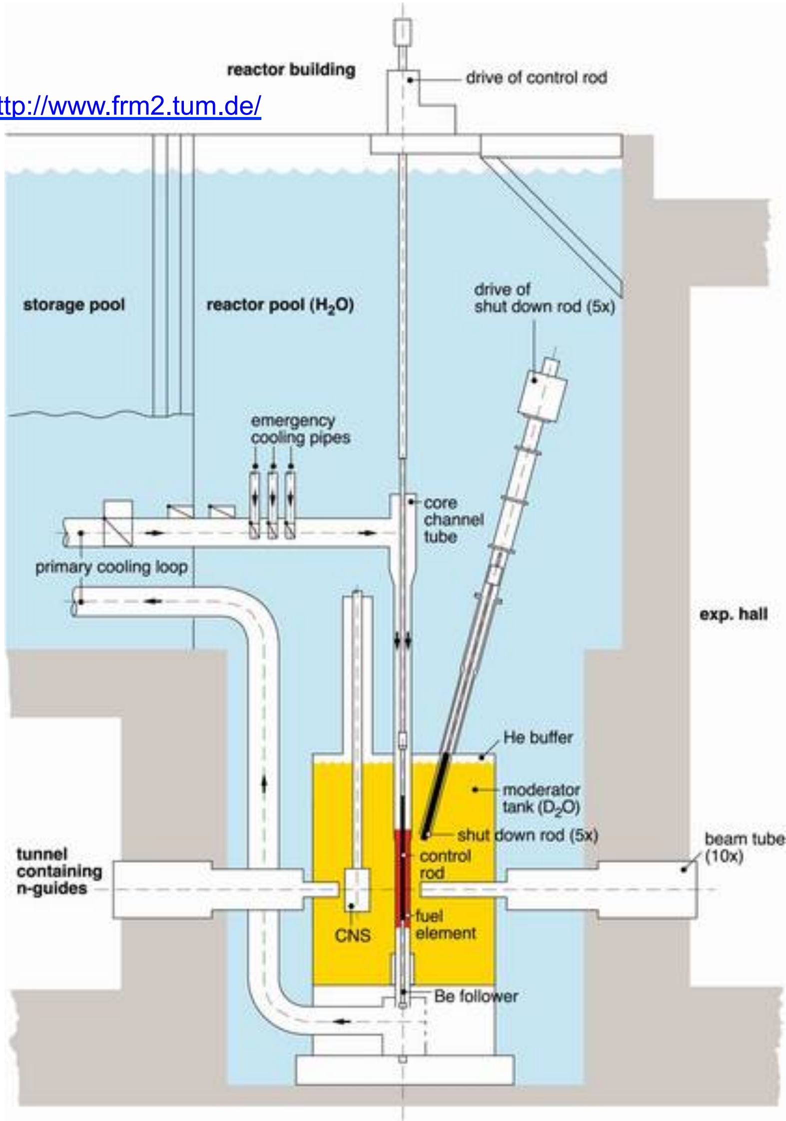

P = 20 MW_{therm}
1 fuel element 8 kg HEU (93% ^{235}U)
neutron flux density: $8 \cdot 10^{14}$ n/(s cm^2)
secondary sources:
unmoderated fission spectrum $2 \cdot 10^{9}$ n/(s cm^2)
Hot neutrons (T = 2400 °C)
cold neutrons (T = 25 K) $9 \cdot 10^{13}$ n/(s cm^2)
Ultracold neutrons (T = 5 K) 10^{6} n/(s cm^2)

Neutron sources at FRM-II of TU Munich

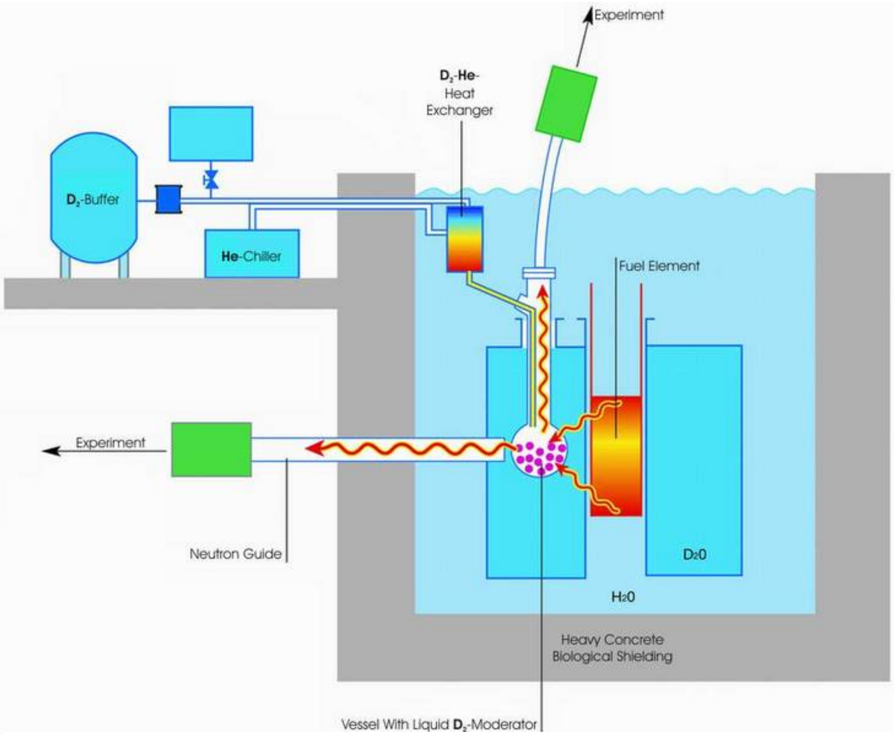

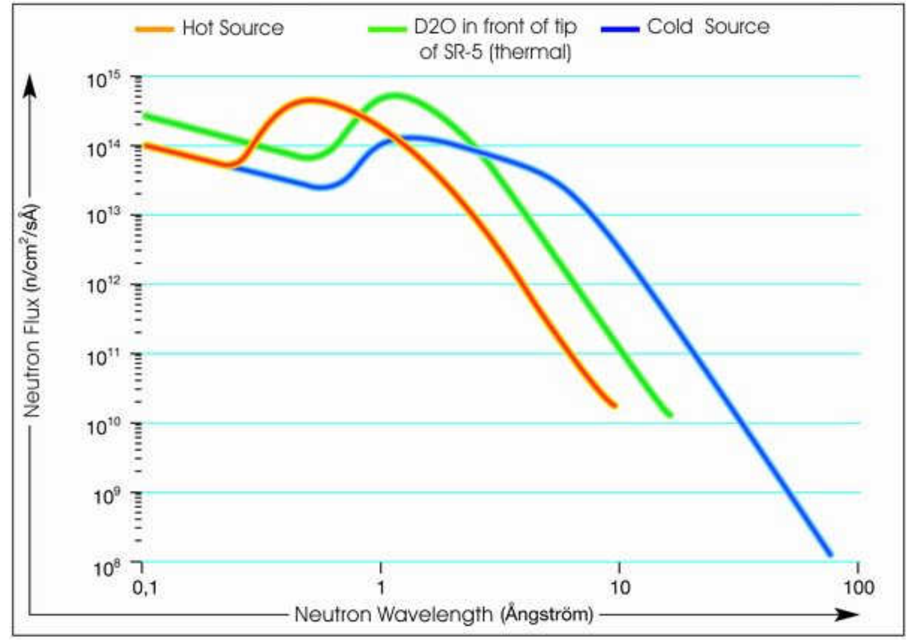

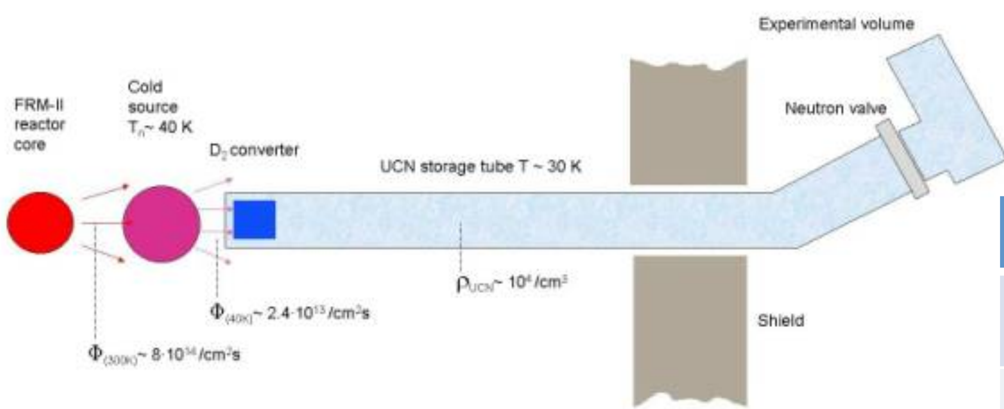

$$\frac{\lambda}{2\pi} = \frac{\hbar}{p} = \frac{\hbar}{\sqrt{2m_n E_{kin} + \frac{E_{kin}^2}{c^2}}}$$

$E\downarrow kin$ (eV)	$\lambda/2\pi$	
0.1	1.44 A	crystal lattice constant
10^6	10 fm	nuclear diameter
10^9	1 fm	Nucleon diameter

Swiss Spallation neutron source SINQ
Paul Scherrer Institute

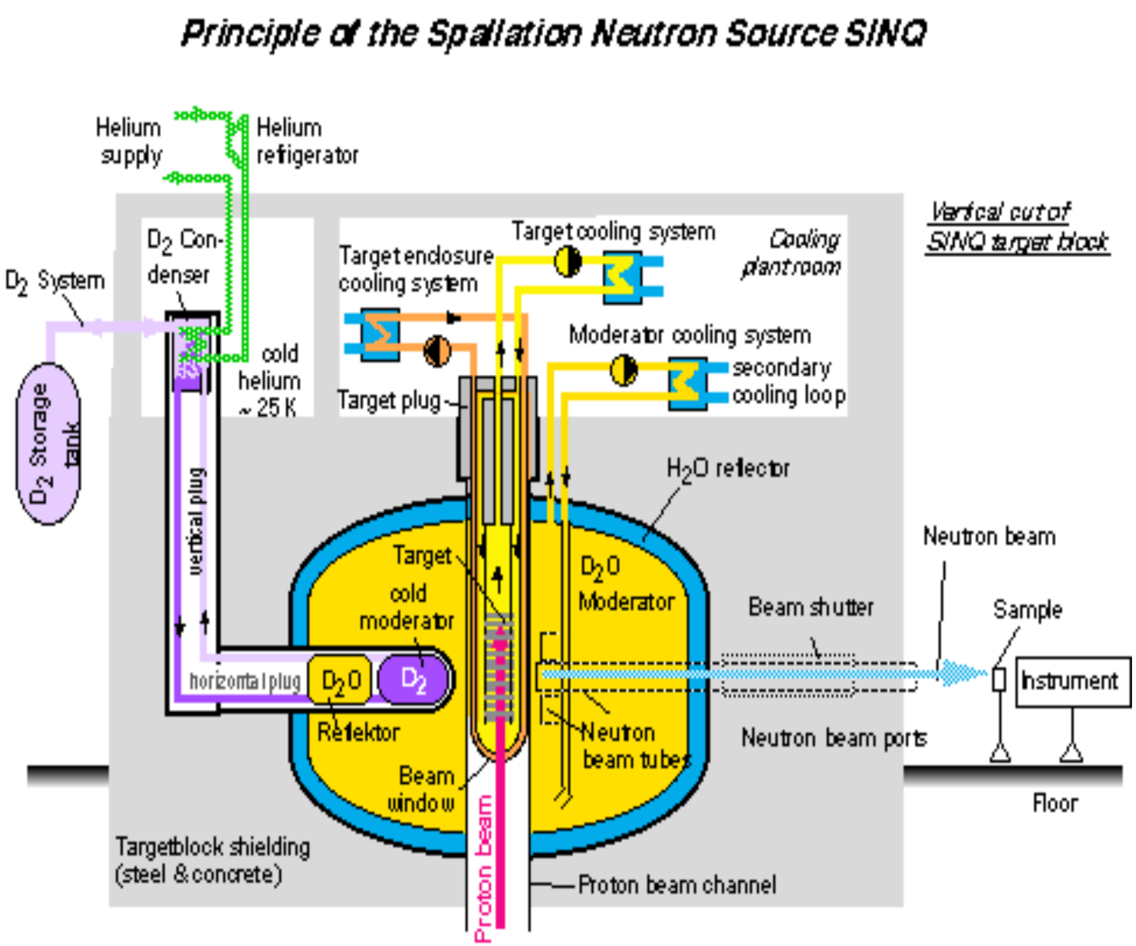

Proton beam 590 MeV, 1.8 mA
beam power ca. 1 MW
for pion production and
proton therapy

Pb spallation target
3-6*10^{16} n/s
moderated and cold source
10^{14} n/(cm^2 s)

Swiss Spallation neutron source SINQ
Paul Scherrer Institute

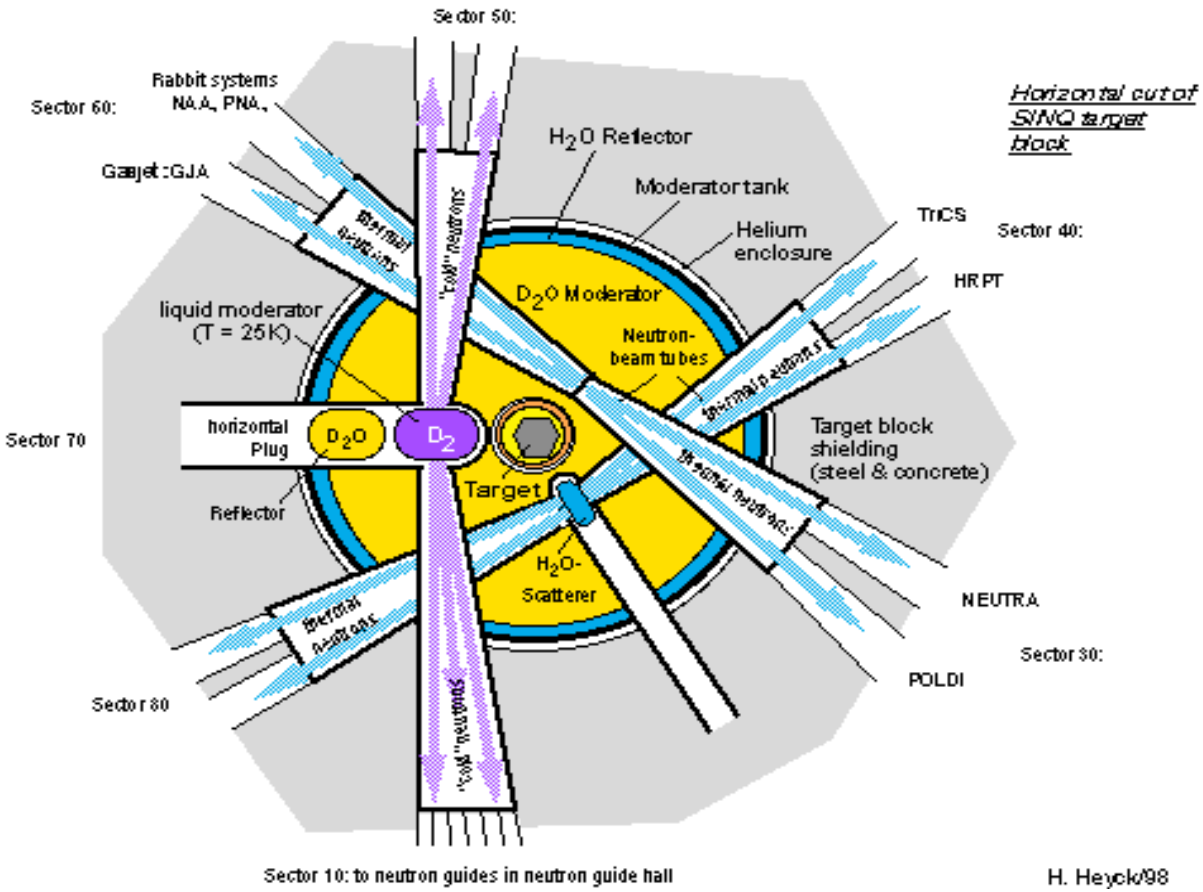

ENDE

Nuclear Transmutation Project

- Roland Beyer, Evert Birgersson**, Anna Ferrari, Roland Hannaske, Mathias Kempe, Toni Kögler, Michele Marta, Ralf Massarczyk, Andrija Matic, Georg Schramm

- Arnd Junghans, Daniel Bemmerer, Eckart Grosse*, Klaus-Dieter Schilling, Ronald Schwengner, Andreas Wagner

- Development of the nELBE photoneutron source together with the Institute for Fluiddynamics and the Central Research Technology Group

  * (also at IKTP Dresden)
  ** now AREVA, Erlangen